FLUXGATE MAGNETOMETER CALIBRATION FOR

MASCOT

MASCOT-MAG-TR-0008

Issue: 1 Revision: 1

January 16, 2014

Protocol and Analysis of the

MASCOT Fluxgate Sensor M1 & FM

Calibration

Dr. Ingo Richter

Institut für Geophysik und extraterrestrische Physik
Technische Universität Braunschweig
Mendelssohnstraße 3, 38106 Braunschweig
Germany

Contents

1 Introduction

This document describes the ground calibration of the MASCOT Fluxgate magnetometer performed at the Magnetsrode Calibration facility operated by the Institute for Geophysics and extraterrestrial Physics, TU Braunschweig.
The tests were executed from January 10 - January 15, 2014.

Part Identification:

Sensor:	M1
Electronics	FM

Key Personnel:

David Hercik:	operating FGM
Ingo Richter:	operating MRode Facility
Reiko Namura:	visiting and assisting

General Setup

- Sensor mounted in thermal box. CoC. Box vertical.
- Sensor Electronics placed in House 2 / Mainroom.
- EGSE placed in House 2 / Mainroom.
- EGSE and Electronics were powered by one single Power Supply in House 2.
  Voltage: +5V / Current: +0.0678A
  Voltage: −5V / Current: -0.0101A
  Voltage: +3.3V / Current: +0.0432A
- Position 1: Standard Alignment
  $X_m = X_c, Y_m = Y_c, Z_m = Z_c$
  Elevation= 0°. Azimuth= 180°.
- Position 2: Turned Position for XY Offset Measurements
  $X_m = -X_c, Y_m = -Y_c, Z_m = Z_c$
  Elevation= 0°. Azimuth= 0°.
- Position 3: Normal Position for Z Offset Measurements
  $X_m = -Z_c, Y_m = -Y_c, Z_m = -X_c$
  Elevation=90°. Azimuth= 0°.
- Position 4: Turned Position for Z Offset Measurements
  $X_m = -Z_c, Y_m = Y_c, Z_m = X_c$
  Elevation=90°. Azimuth= 180°.

- The pictures were taken before rotating the box to the vertical orientation.
- TEMPCTRL-Parameters for Heating:
  Field-Active-Time: 25s
  SOL controlled, Delay after SOL: 8s
  Max. Heating Time: 20s
  Heating-Profile: *manual*
  Heater-Select: automatic
  Smart_heat: on
- TEMPCTRL-Parameters for Cooling:
  Field-Active-Time: 25s
  SOL controlled, Delay after SOL: 8s
  Max. Cooling Time: 8s
  Heating-Profile: *manual*
  Heater-Select: *automatic*
  Smart_heat: *on*
- IP-Adressses:
  EGSE: 192.168.124.40
  Terminal: 192.168.124.50
- MRode-Terminal software:
  TERMINAL_17_MASCOT.vi
- DUT parameters:
  Phase X: 104
  Phase Y: 107
  Phase Z: 109
  Samplerate: 10 Hz
- The MCF has been calibrated electrically and geometrically in the weeks just before the MASCOT calibration.
  The results are described in the report MR-IGEP-TR-1009.

<u>REMARKS:</u>

- **The Analysis has been performed using a nominal conversion factor of 1.0 nT/ADCcounts.**
- **All values (e.g Offsets) given in engineering nanotesla (enT) have to be multiplied with the calculated sensitivities to obtain real nanotesla values.**

Standard Sensor Setup:

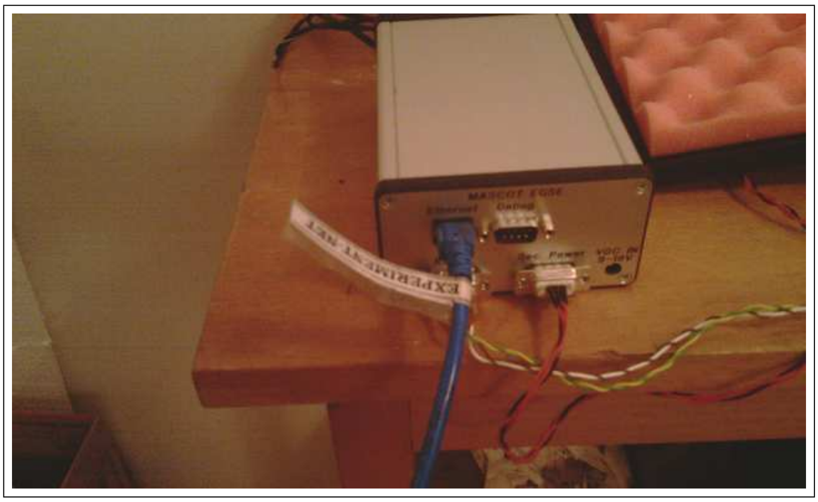

Figure 1: The MASCOT EGSE in House 2

Figure 2: The FM electronics board in House 2

Figure 3: The M1 sensor mounted in the thermal box in POSITION 1 , view from top

Figure 4: The M1 sensor mounted in the thermal box in POSITION 1 , view from south

2 Measurements on January 10, 2014

The MASCOT equipment was shipped to MRode and everything was installed in the afternoon. The sensor was mounted to the brown sensor plate and placed in the thermal box. The electronics and EGSE was put on the small desk near the coilsystem. The sensor was rotated to POSITION 1.
First test of the system at 15:30.

Initial Reading of the thermistors:

T_{59}	=	16.6°C
T_{ELEC}	=	21.23°C
T_{SENS}	=	20.44°C

A first test of the M1 Sensor revealed the correct soldering of the components. Application of 10000 nT fields in all main axes in Standard orientation yielded:

X_{m}	=	X_{c}
Y_{m}	=	Y_{c}
Z_{m}	=	Z_{c}

2.1 Data

CCD File	Configuration File	Remark
14-01-10\16-25-52.CCR	OFFSET_200.MAG	
14-01-10\16-35-17.CCR	NULL.MAG	
14-01-10\16-35-54.CCR	NULL.MAG	
14-01-10\16-36-30.CCR	LIN11000XYZ.MAG	
14-01-10\17-07-01.CCR	LIN11000XYZ.MAG	
14-01-10\17-37-32.CCR	LIN11000XYZ.MAG	
14-01-10\18-08-03.CCR	LIN11000XYZ.MAG	
14-01-10\18-38-35.CCR	LIN11000XYZ.MAG	
14-01-10\19-09-06.CCR	LIN11000XYZ.MAG	
14-01-10\19-39-37.CCR	LIN11000XYZ.MAG	
14-01-10\20-10-07.CCR	LIN11000XYZ.MAG	
14-01-10\20-40-39.CCR	LIN11000XYZ.MAG	
14-01-10\21-11-09.CCR	LIN11000XYZ.MAG	
14-01-10\21-41-40.CCR	LIN11000XYZ.MAG	
14-01-10\22-12-11.CCR	NULL.MAG	

2.2 DC-Analysis at Environmental Temperature

A standard linearity and offset measurement was performed at 16°C.

2.2.1 Calibration on 3 Linear Axes

Used Files:

CCD File	Configuration File	Remark
14-01-10\17-37-32.CCR	LIN11000XYZ.MAG	

Parameter File: `PARAMETER_LIN__14-01-10_17-37-32.CPF`

Facility Parameter:

Nominal Sensor Setup $\underline{B}_{\text{DUT}} = \underline{\underline{R}}_{\text{nom}} \underline{B}_{\text{c}}$

$$\underline{\underline{R}}_{\text{nom}} = \begin{pmatrix} +1.000000 & +0.000000 & +0.000000 \\ +0.000000 & +1.000000 & +0.000000 \\ +0.000000 & +0.000000 & +1.000000 \end{pmatrix}$$

Calculated Sensor Rotation:

$$\underline{\underline{\rho}} = \begin{pmatrix} +0.999545 & +0.008286 & +0.028999 \\ -0.008137 & +0.999953 & -0.005235 \\ -0.029041 & +0.004996 & +0.999566 \end{pmatrix}$$

Rotation Angles:

$$\begin{aligned} \text{Angle } (X_c, X_m): \quad & \lambda_{\text{x}} = +1^\circ\ 43'42'' \\ \text{Angle } (Y_c, Y_m): \quad & \mu_{\text{y}} = +0^\circ\ 33'16'' \\ \text{Angle } (Z_c, Z_m): \quad & \nu_{\text{z}} = +1^\circ\ 41'19'' \end{aligned}$$

Determinant of Rotation Matrix: 1.00000
Nominal Field Source: SOLARTRON
Fields applied for 24.0 s
Mean Sensor Temperature: 16.6°C
Automatic Coil Correction: used

Earthfield Compensation:	X	=	DYNAMIC
	Y	=	DYNAMIC
	Z	=	DYNAMIC

Offset Treatment:

A polynomial offset trend of order 2 has been fitted and subtracted from the raw data before creating the sensor model.

Mean Coil System Residual + Sensor Offset: $\underline{B}^{or}$ = (21.089 , 11.377 , -4.858) nT

Raw Data Quality:

Standard Deviation of used Raw Data Blocks:

[Values in eng nT]	s_x	s_y	s_z
Minimum	0.020	0.017	0.015
Mean	0.059	0.045	0.052
Maximum	0.150	0.114	0.147

Calibration Parameter:

$$\text{Transfermatrix:}\quad \underline{\underline{\phi}} = \underline{\underline{R}}_{\text{nom}}\,\underline{\underline{\rho}}\,\underline{\underline{\omega}}\,\underline{\underline{\sigma}} = \begin{pmatrix} +0.997848 & +0.008339 & +0.028972 \\ -0.013611 & +0.999085 & -0.005230 \\ -0.034122 & +0.007074 & +0.998655 \end{pmatrix}$$

$$\text{Reduced Transfermatrix:}\quad \underline{\underline{\tilde{\phi}}} = \underline{\underline{\omega}}\,\underline{\underline{\sigma}} = \begin{pmatrix} +0.998496 & +0.000000 & +0.000000 \\ -0.005513 & +0.999142 & +0.000000 \\ -0.005100 & +0.002083 & +0.999089 \end{pmatrix}$$

$$\text{Sensitivity:}\quad \underline{\underline{\sigma}} = \begin{pmatrix} +0.998496 & +0.000000 & +0.000000 \\ +0.000000 & +0.999127 & +0.000000 \\ +0.000000 & +0.000000 & +0.999074 \end{pmatrix}$$

$$\text{Misalignment:}\quad \underline{\underline{\omega}} = \begin{pmatrix} +1.000000 & +0.000000 & +0.000000 \\ -0.005522 & +1.000015 & +0.000000 \\ -0.005107 & +0.002085 & +1.000015 \end{pmatrix}$$

Sensor Misalignment Angles:

$$\begin{aligned} \xi_{\text{x,y}} &= +89^\circ\ 41'1'' \\ \xi_{\text{x,z}} &= +89^\circ\ 42'29'' \\ \xi_{\text{y,z}} &= +90^\circ\ 7'4'' \end{aligned}$$

Model Quality:

Standard Deviation, Maximum and Minimum Error of Calculated Model:

[Values in nT]	X	Y	Z
Standard Deviation	0.319	0.112	0.678
Maximum Error	0.815	0.214	1.614
Minimum Error	-0.867	-0.418	-0.963

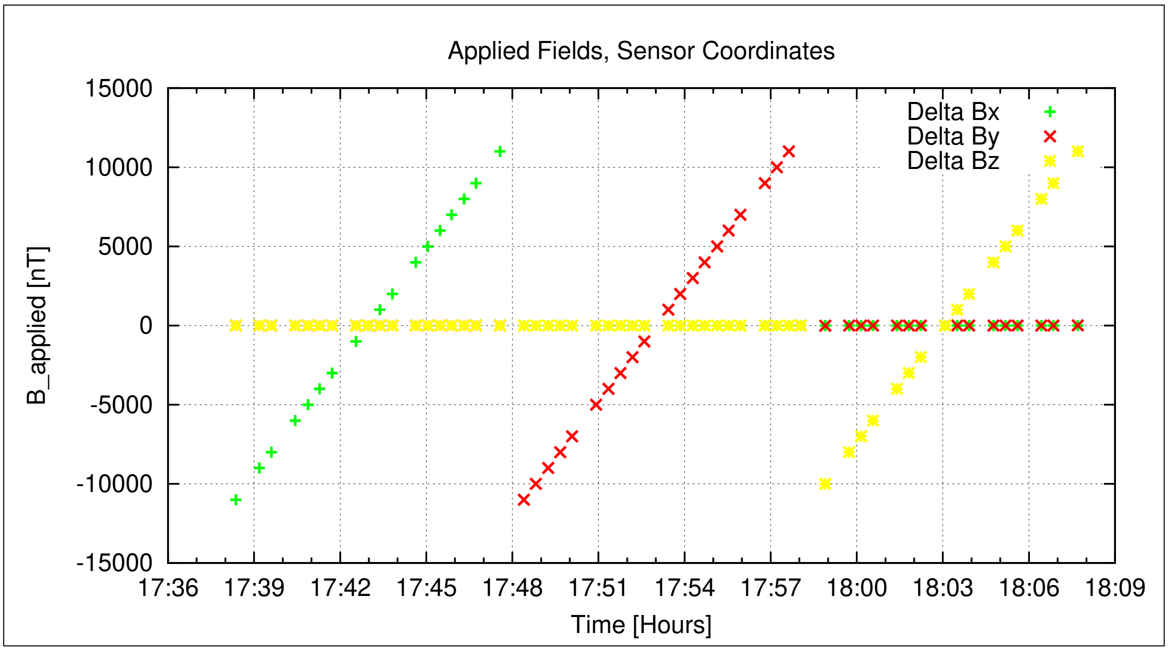

Figure 5: Applied Fields

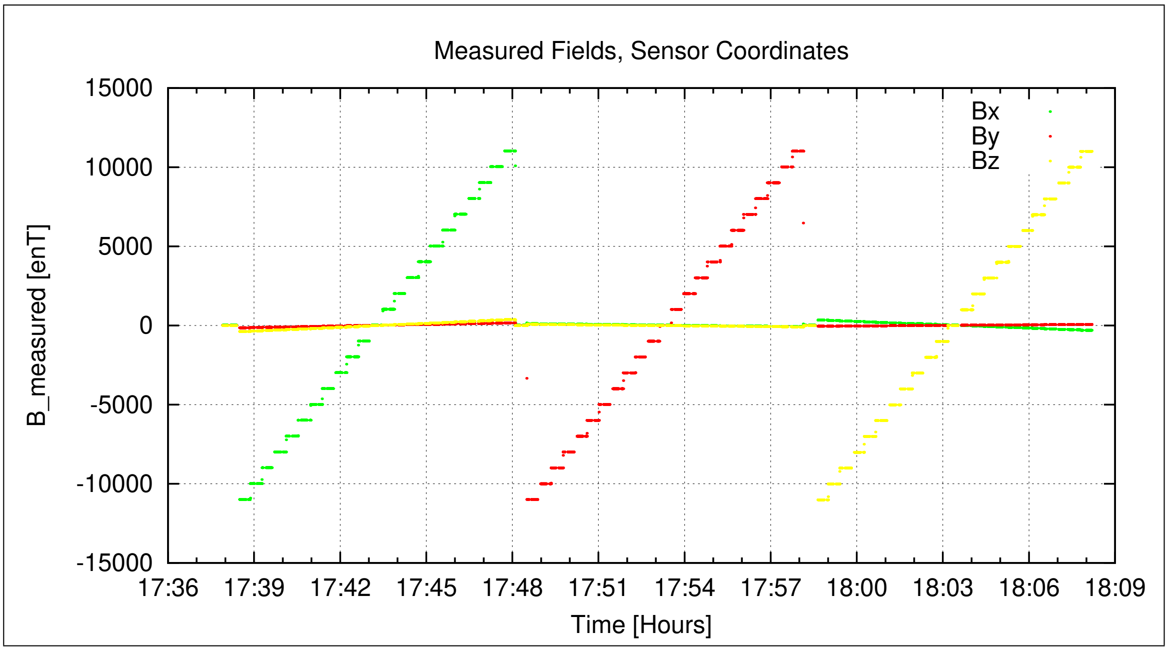

Figure 6: Measured Data

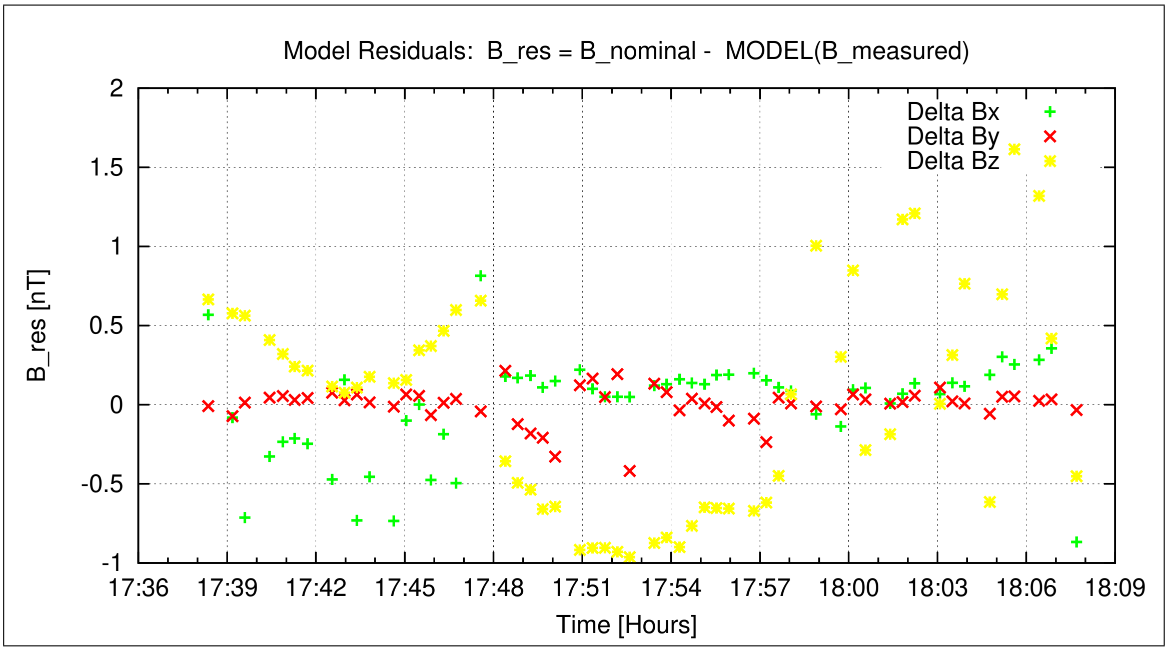

Figure 7: Model Quality - Differences of applied field and modelled measurement data

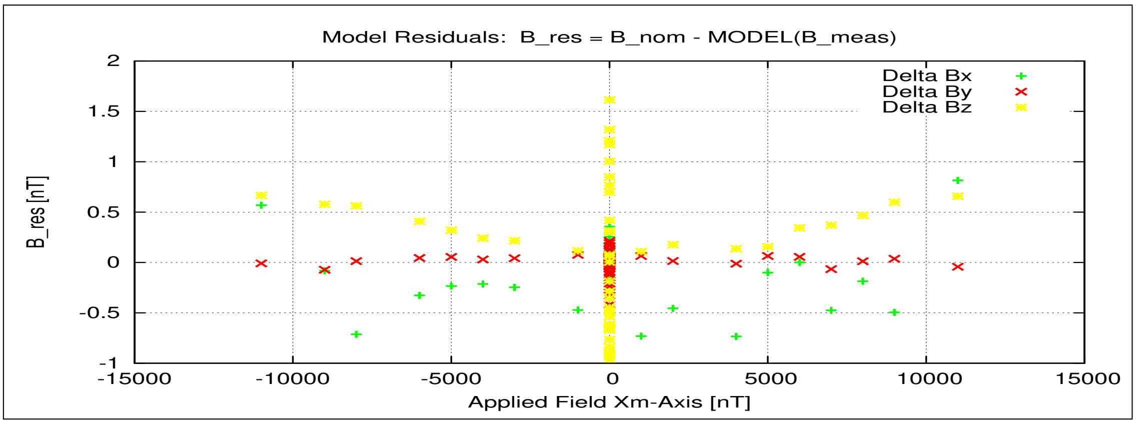

Figure 8: RESIDUALS vs FLD X

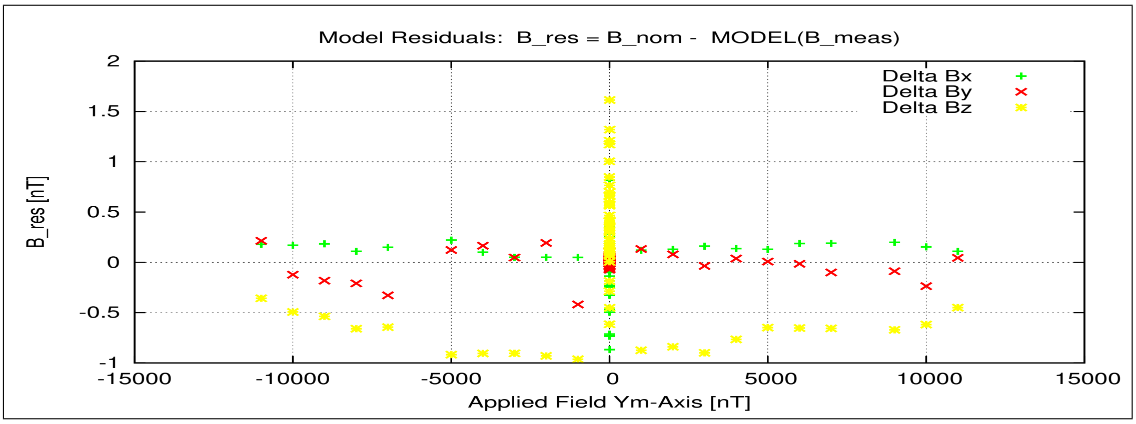

Figure 9: RESIDUALS vs FLD Y

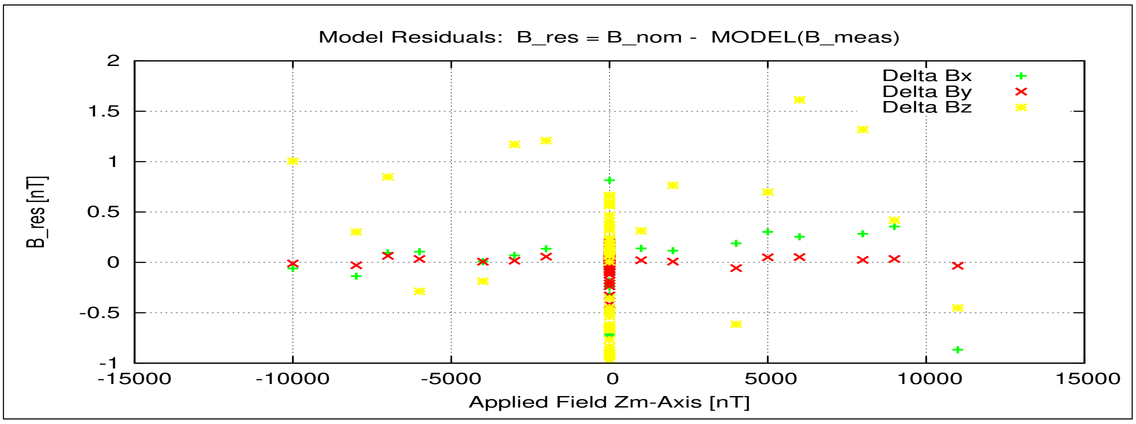

Figure 10: RESIDUALS vs FLD Z

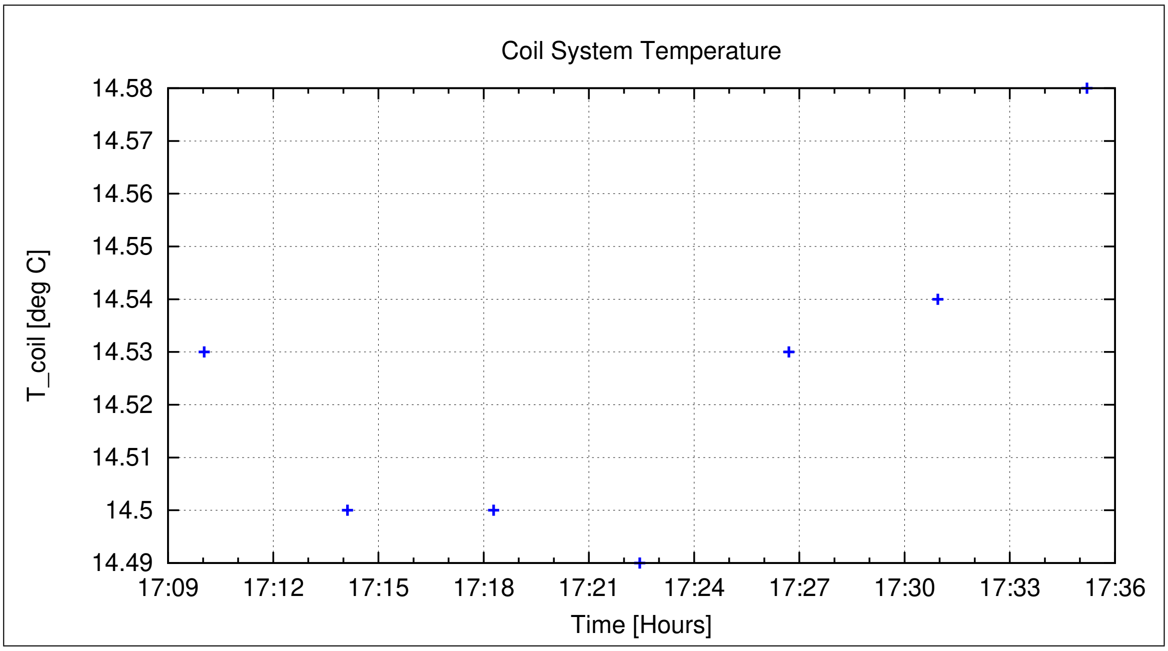

Figure 11: Coil System Temperature

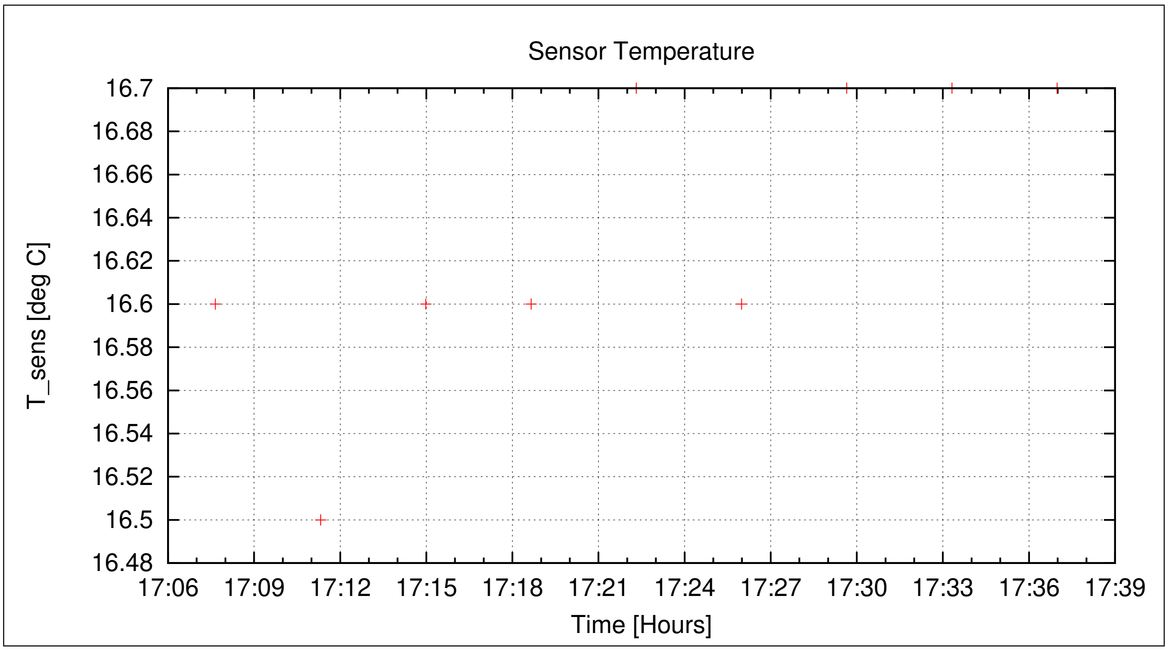

Figure 12: Sensor Temperature

2.2.2 OFFSET Calculation

In this section the instrument offsets and the residual field of the Coil System will be evaluated. Measurements at two orientations for each component act as input for the offset calculation. From the "normal" (0-degrees) and "turned" (180-degrees) orientations the offsets and residual fields can be derived:

$$B_{\text{off}} = \frac{B_{\text{normal}} + B_{\text{turned}}}{2}$$
$$B_{\text{res}} = \frac{B_{\text{normal}} - B_{\text{turned}}}{2}$$

Used Offset Measurements:

CCD File	Configuration File	Remark
14-01-10\16-25-52.CCR	OFFSET_200.MAG	

Parameter File: OFF_PARAMETER__14-01-10-16-25-52.OPF

Calibration Parameter:

Sensor Offsets:

Component	Offset [enT]	Standard deviation [enT]
X	19.58	0.084
Y	13.23	0.117
Z	7.75	0.082

Residual Field of the Coil System:

Component	B_{res} [enT]
X	3.19
Y	-2.26
Z	-1.76

Remark: Residual field is given in actual DUT coordinates, not in coil-coordinates!

Zerofield measurements in dynamically compensated earthfield conditions were conducted during the night and for the weekend.

3 Measurements on January 11, 2014

No personnel around today. Zerofield measurements continued.

3.1 Data

CCD File	Configuration File	Remark
14-01-11\10-12-31.CCR	NULL.MAG	
14-01-11\22-12-51.CCR	NULL.MAG	

Remark:

Due to an unknown error the data transmission from the EGSE to the MRode CDRS stopped at about 22:00. Therefore, no further data are available from this weekend.

4 Measurements on January 12, 2014

No personnel around today. Zerofield measurements continued but no MAG data were collected.

4.1 Data

CCD File	Configuration File	Remark
14-01-12\10-13-11.CCR	NULL.MAG	
14-01-12\22-13-31.CCR	NULL.MAG	

5 Measurements on January 13, 2014

The cooling system was activated at 07:42. The first temperature goal was set to -10°C. The pressurizing system was not used, as the LN2-vessel has been already installed 3 days ago and the internal pressure was at the necessary level of 0.4 bar.

5.1 Data

CCD File	Configuration File	Remark
14-01-13\07-29-31.CCR	NULL.MAG	
14-01-13\07-42-04.CCR	LIN11000XYZ.MAG	
14-01-13\08-12-34.CCR	LIN11000XYZ.MAG	
14-01-13\08-43-55.CCR	OFFSET_200.MAG	
14-01-13\08-52-32.CCR	LIN11000XYZ.MAG	
14-01-13\09-23-03.CCR	LIN11000XYZ.MAG	
14-01-13\09-53-35.CCR	LIN11000XYZ.MAG	
14-01-13\10-25-04.CCR	OFFSET_200.MAG	
14-01-13\10-32-53.CCR	LIN11000XYZ.MAG	
14-01-13\11-03-25.CCR	LIN11000XYZ.MAG	
14-01-13\11-33-56.CCR	LIN11000XYZ.MAG	
14-01-13\12-04-27.CCR	LIN11000XYZ.MAG	
14-01-13\12-34-58.CCR	LIN11000XYZ.MAG	
14-01-13\13-05-30.CCR	LIN11000XYZ.MAG	
14-01-13\13-36-00.CCR	LIN11000XYZ.MAG	
14-01-13\14-10-49.CCR	OFFSET_200.MAG	
14-01-13\14-24-29.CCR	FREQ10000.MAG	
14-01-13\15-10-49.CCR	LIN11000XYZ.MAG	
14-01-13\15-41-19.CCR	LIN11000XYZ.MAG	
14-01-13\16-11-49.CCR	LIN11000XYZ.MAG	
14-01-13\16-42-19.CCR	LIN11000XYZ.MAG	
14-01-13\17-12-49.CCR	LIN11000XYZ.MAG	
14-01-13\17-43-19.CCR	LIN11000XYZ.MAG	
14-01-13\18-13-50.CCR	LIN11000XYZ.MAG	
14-01-13\18-44-21.CCR	LIN11000XYZ.MAG	
14-01-13\19-14-52.CCR	LIN11000XYZ.MAG	
14-01-13\19-45-22.CCR	LIN11000XYZ.MAG	
14-01-13\20-15-53.CCR	LIN11000XYZ.MAG	
14-01-13\20-46-24.CCR	LIN11000XYZ.MAG	
14-01-13\21-16-56.CCR	LIN11000XYZ.MAG	
14-01-13\21-47-27.CCR	LIN11000XYZ.MAG	
14-01-13\22-17-57.CCR	LIN11000XYZ.MAG	
14-01-13\22-48-27.CCR	LIN11000XYZ.MAG	
14-01-13\23-18-58.CCR	LIN11000XYZ.MAG	
14-01-13\23-49-28.CCR	LIN11000XYZ.MAG	

5.2 DC-Analysis at Moderate Low Temperature

Linearity and offset measurements were performed at $T_{59} = -12°\mathrm{C}$.

Thermal Analysis: refer to section 8.

Afterwards the DUT was cooled down to $\sim -40°\mathrm{C}$.

5.3 DC-Analysis at Low Temperature

Linearity and offset measurements were performed at $T_{59} = -41°\mathrm{C}$.

Thermal Analysis: refer to section 8.

Afterwards the DUT was cooled down further to $\sim -80°\mathrm{C}$.

5.4 DC-Analysis at Very Low Temperature

Linearity and offset measurements were performed at $T_{59} = -85°\mathrm{C}$.

Thermal Analysis: refer to section 8.

Afterwards the heating and cooling system was switched off. Linearity measurements in dynamically compensated earthfield conditions were performed during the night. These measurements started at 15:10.

6 Measurements on January 14, 2014

07:40 inspection of the system. Everything was ok. The linearity measurement was stopped. The system was at a temperature of $T_{59} = -18.1°$.

6.1 Data

CCD File	Configuration File	Remark
14-01-14\00-19-59.CCR	LIN11000XYZ.MAG	
14-01-14\00-50-30.CCR	LIN11000XYZ.MAG	
14-01-14\01-20-59.CCR	LIN11000XYZ.MAG	
14-01-14\01-51-29.CCR	LIN11000XYZ.MAG	
14-01-14\02-21-59.CCR	LIN11000XYZ.MAG	
14-01-14\02-52-29.CCR	LIN11000XYZ.MAG	
14-01-14\03-22-59.CCR	LIN11000XYZ.MAG	
14-01-14\03-53-29.CCR	LIN11000XYZ.MAG	
14-01-14\04-24-00.CCR	LIN11000XYZ.MAG	
14-01-14\04-54-30.CCR	LIN11000XYZ.MAG	
14-01-14\05-25-02.CCR	LIN11000XYZ.MAG	
14-01-14\05-55-33.CCR	LIN11000XYZ.MAG	
14-01-14\06-26-04.CCR	LIN11000XYZ.MAG	
14-01-14\06-56-35.CCR	LIN11000XYZ.MAG	
14-01-14\07-27-06.CCR	LIN11000XYZ.MAG	
14-01-14\07-41-16.CCR	OFFSET_200.MAG	
14-01-14\07-53-39.CCR	LIN11000XYZ.MAG	
14-01-14\09-53-24.CCR	LIN11000XYZ.MAG	
14-01-14\10-24-51.CCR	OFFSET_200.MAG	
14-01-14\10-32-56.CCR	FREQ10000.MAG	
14-01-14\11-18-08.CCR	LIN11000XYZ.MAG	
14-01-14\11-48-38.CCR	LIN11000XYZ.MAG	
14-01-14\12-19-09.CCR	LIN11000XYZ.MAG	
14-01-14\12-49-39.CCR	LIN11000XYZ.MAG	
14-01-14\13-21-06.CCR	OFFSET_200.MAG	
14-01-14\13-28-50.CCR	FREQ10000.MAG	
14-01-14\14-12-05.CCR	LIN11000XYZ.MAG	
14-01-14\14-42-36.CCR	LIN11000XYZ.MAG	
14-01-14\15-13-07.CCR	LIN11000XYZ.MAG	
14-01-14\15-44-27.CCR	OFFSET_200.MAG	
14-01-14\15-57-46.CCR	FREQ10000.MAG	
14-01-14\16-43-36.CCR	LIN11000XYZ.MAG	
14-01-14\17-14-07.CCR	LIN11000XYZ.MAG	
14-01-14\17-44-37.CCR	LIN11000XYZ.MAG	
14-01-14\18-15-07.CCR	LIN11000XYZ.MAG	
14-01-14\18-45-37.CCR	LIN11000XYZ.MAG	
14-01-14\19-16-08.CCR	LIN11000XYZ.MAG	
14-01-14\19-46-39.CCR	LIN11000XYZ.MAG	
14-01-14\20-17-10.CCR	LIN11000XYZ.MAG	

```
14-01-14\20-47-40.CCR      LIN11000XYZ.MAG
14-01-14\21-18-11.CCR      LIN11000XYZ.MAG
14-01-14\21-48-42.CCR      LIN11000XYZ.MAG
14-01-14\22-19-12.CCR      NULL.MAG
```

6.2 DC-Analysis at Moderate low Temperature

Linearity and offset measurements were performed at $T_{59} = -18.1°C$.

Thermal Analysis: refer to section 8.

Afterwards the heating system was activated and the sensor was heated up to $T_{59} = 40.1°C$.

6.3 DC-Analysis at Moderate High Temperature

Linearity and offset measurements were performed at $T_{59} = +41.5°C$.

Thermal Analysis: refer to section 8.

6.4 AC-Analysis at Moderate High Temperature

A frequency measurement was performed at 40°C.

Setup:

- Sensor mounted in thermal box. CoC. Box vertical.
- Sensor rotated to:
  Elevation= 45°
  Azimuth= 126°
- Field applied on Y_c.
- No attenuator

6.4.1 Frequency Measurements

This section is dedicated to the frequency behavior of the instrument. The analysis of the performed AC measurements allows to calculate the actual sampling frequency f_s of the instrument and the frequency response (amplitude vs. frequency). The measurements have been performed with the sensor placed at CoC in a diagonal in space orientation. The AC-fields have been applied on the Y_c axis only. Using this setup it can be guaranteed that only one frequency is applied at a time and no beat effects occur.

Used Frequency Measurements:

CCD File	Configuration File	Remark
`14-01-14\10-32-56.CCR`	`FREQ10000.MAG`	

Parameter File: `FREQ_PARAMETER__14-01-14-10-32-56.FPF`

Calibration Parameter:

Sampling Frequency:

Component	f_s [Hz]	Standard deviation [Hz]
X	10.0000	0.000280
Y	10.0002	0.001927
Z	10.0000	0.000183
Mean Sampling Frequency	10.0001	0.000137

3 dB Corner Frequency:

Component	f_{3dB} [Hz]
X	5.10
Y	4.86
Z	5.02

Applied Frequencies and Measured Amplitudes

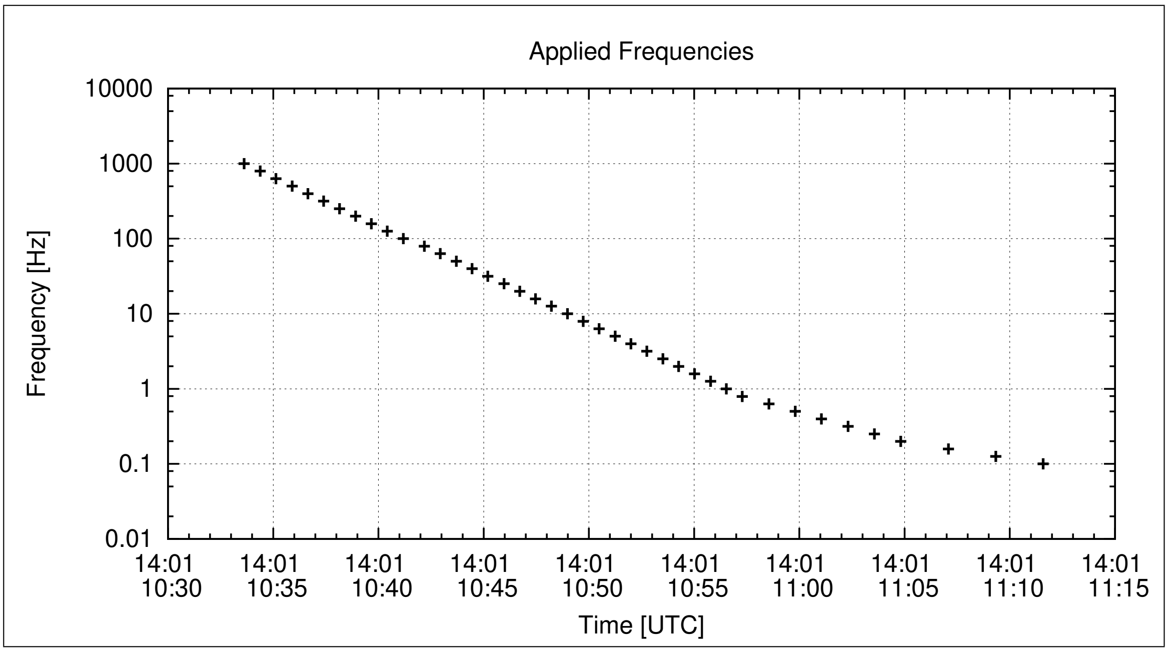

Figure 13: Applied Frequencies for AC Analysis

Applied Frequency [Hz]	Bx [enT]	By [enT]	Bz [enT]
1000.000	56.40	46.53	12.87
794.000	49.94	53.28	38.90
631.000	0.24	0.28	0.21
501.000	123.54	142.58	105.37
398.000	145.21	165.63	125.28
316.000	0.34	0.01	0.74
251.000	11.08	6.47	10.19
199.000	180.88	207.36	158.85
158.000	35.93	21.12	33.54
126.000	58.84	39.06	55.08
100.000	156.03	164.30	134.31
79.400	28.17	20.19	26.09
63.100	130.06	78.57	123.03
50.100	4.72	13.17	4.90
39.800	14.07	10.64	13.69
31.600	134.65	81.83	132.13
25.100	366.28	234.86	354.38
19.900	15.85	22.38	15.23
15.800	601.80	459.66	563.54
12.600	572.71	481.01	533.21
10.000	3.07	9.98	2.95
7.900	760.07	716.58	712.85
6.310	1415.80	1359.88	1332.22
5.010	1276.39	1666.50	1179.30
3.980	2314.06	2246.80	2184.03
3.160	2568.45	2496.81	2425.86
2.510	2736.91	2662.12	2586.13
1.990	2846.54	2769.88	2690.21
1.580	2915.77	2837.89	2756.41
1.260	2960.84	2882.30	2798.71
1.000	2989.50	2910.35	2825.43
0.790	3010.13	2930.76	2845.63
0.631	3021.35	2941.76	2856.27
0.501	3027.98	2948.18	2862.29
0.398	3032.83	2953.37	2867.68
0.316	3035.81	2956.16	2869.97
0.251	3036.34	2956.43	2870.48
0.199	3038.82	2959.12	2872.76
0.158	3039.24	2959.82	2873.04
0.126	3040.36	2960.71	2874.31
0.100	3039.45	2959.87	2872.96

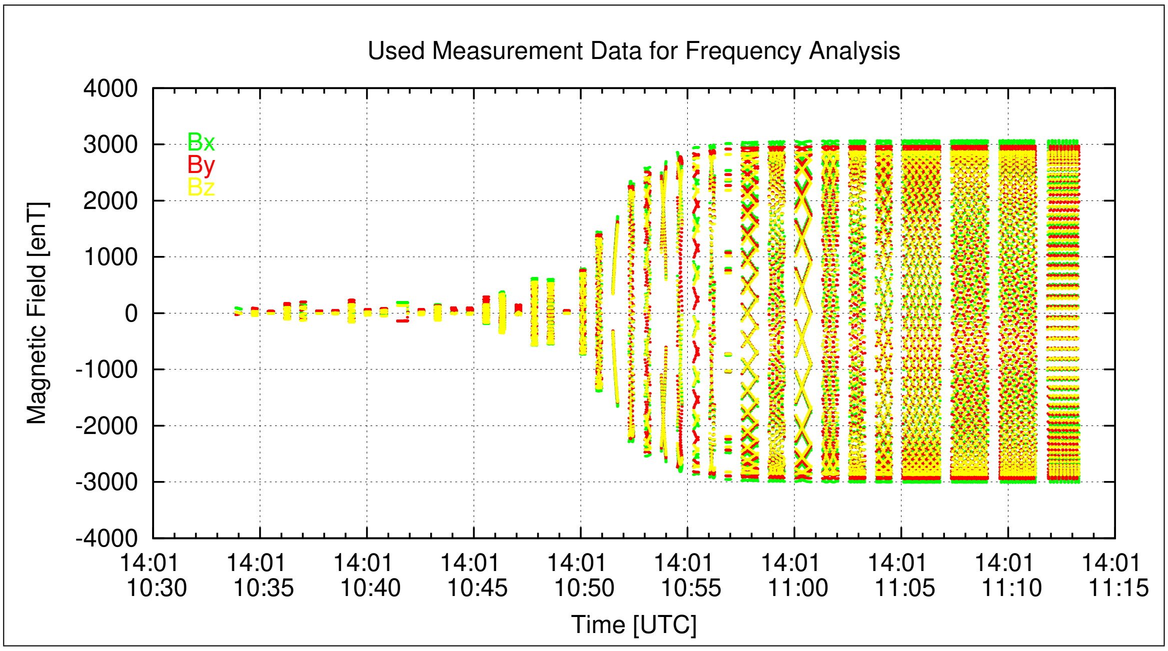

Figure 14: Used packets of Measured data for the Frequency analysis

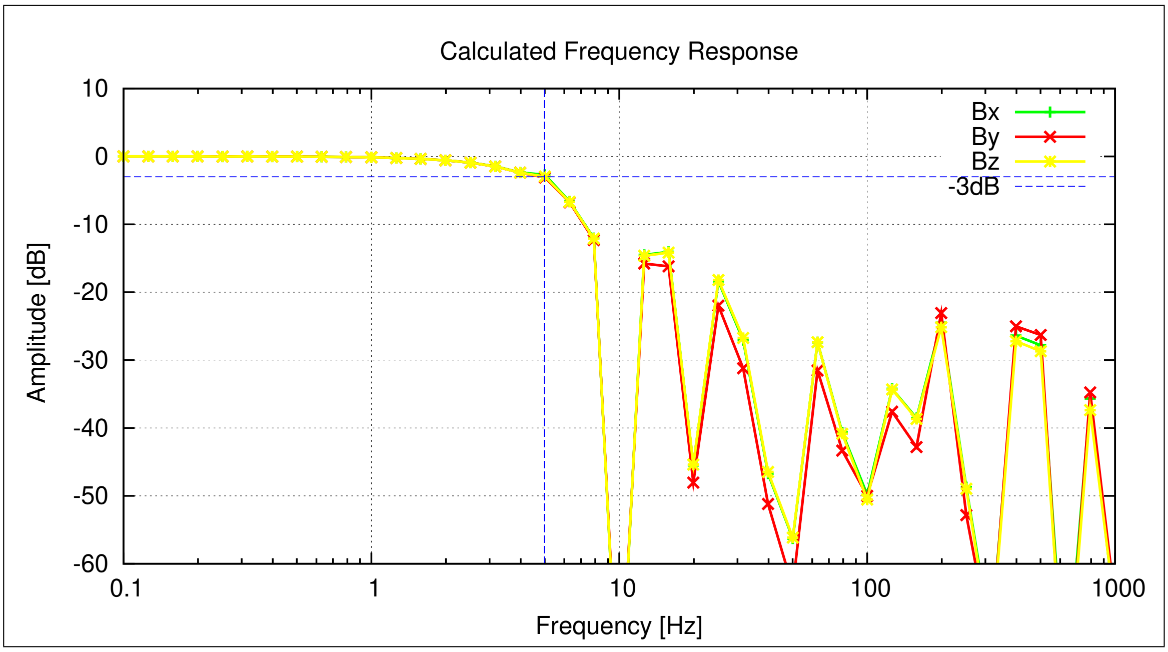

Figure 15: Calculated Frequency Response

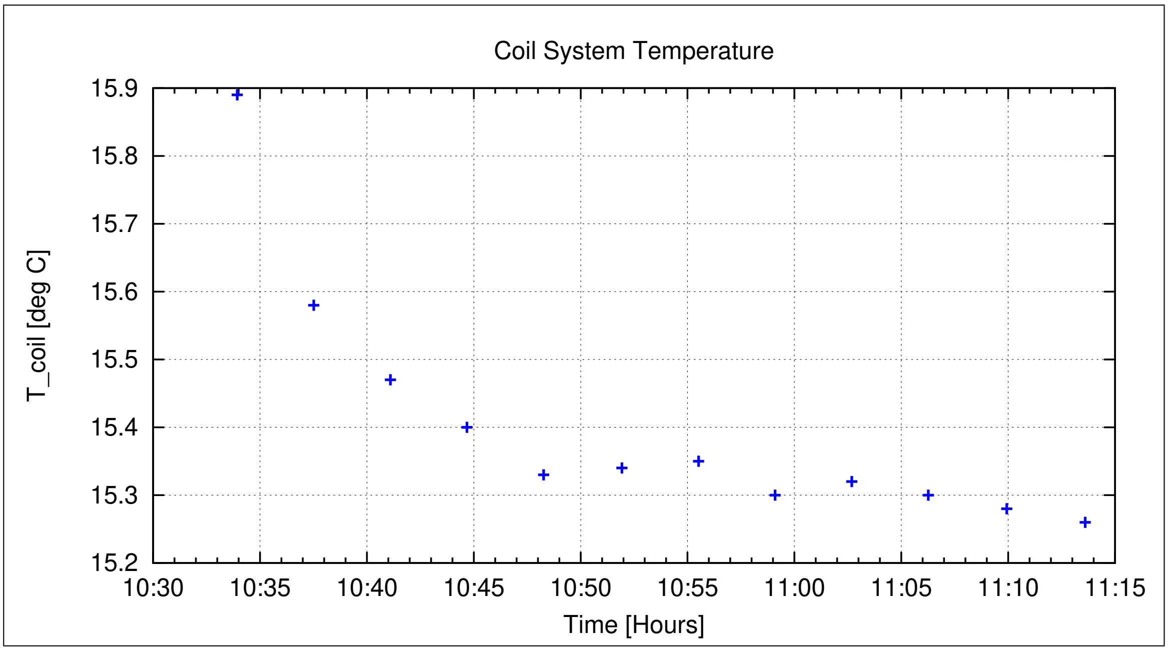

Figure 16: Coil System Temperature

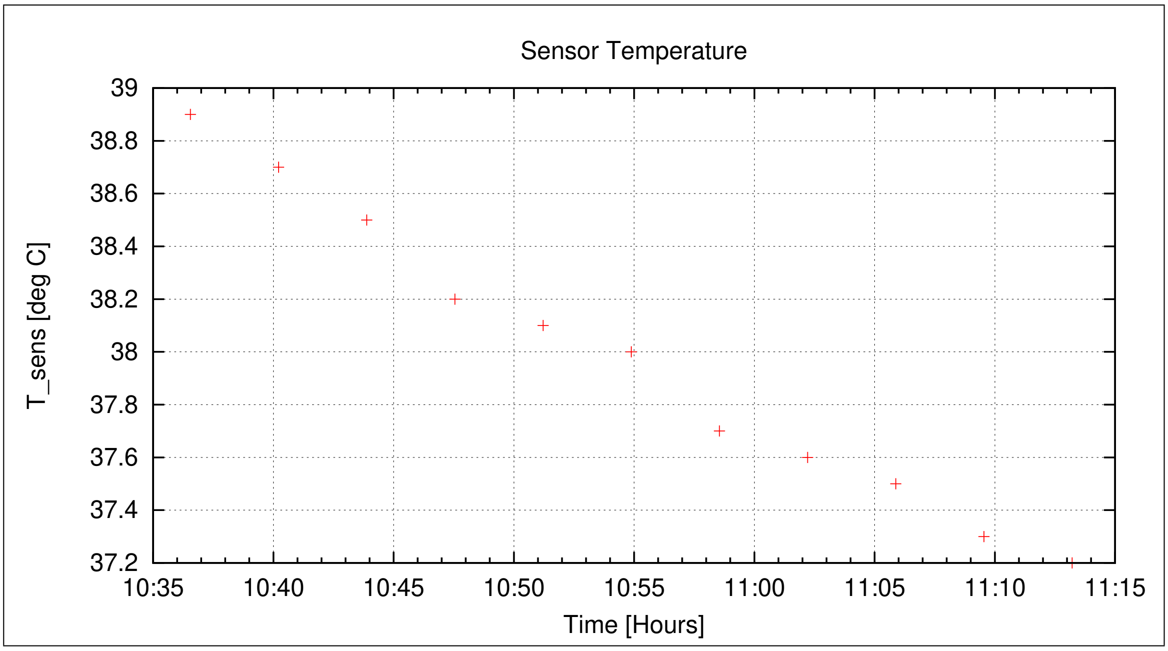

Figure 17: Sensor Temperature

Afterwards the sensor was heated up to $T_{59} = +60°C$.

6.5 DC-Analysis at High Temperature

Linearity and offset measurements were performed at $T_{59} = +60°C$.

Thermal Analysis: refer to section 8.

6.6 AC-Analysis at High Temperature

A frequency measurement was performed at 60°C.

Thermal Analysis: refer to section 8.

Afterwards the sensor was heated up to $T_{59} = +80°C$.

6.7 DC-Analysis at Very High Temperature in Turned Configuration

The sensor was rotated to POSITION 4, to be able to see, whether the slightly worse performance of the z-component is related to the DUT or to the MCF. Analysis of the conducted linearity measurement showed, that the performance of the z-component stays constant. The effect rotates with the sensor; this means that the MCF works properly and the DUT has different properties on x,y and the z-axis (higher residuals on the model fits for the z-axis.)

This linearity measurement was performed at 80°C.

6.7.1 Calibration on 3 Linear Axes

Used Files:

CCD File	Configuration File	Remark
14-01-14\14-42-36.CCR	LIN11000XYZ.MAG	

Parameter File: `PARAMETER_LIN__14-01-14_14-42-36.CPF`

Facility Parameter:

Nominal Sensor Setup $\underline{B}_{\text{DUT}} = \underline{\underline{R}}_{\text{nom}} \underline{B}_{\text{c}}$

$$\underline{\underline{R}}_{\text{nom}} = \begin{pmatrix} +0.000000 & +0.000000 & -1.000000 \\ +0.000000 & +1.000000 & +0.000000 \\ +1.000000 & +0.000000 & +0.000000 \end{pmatrix}$$

Calculated Sensor Rotation:

$$\underline{\underline{\rho}} = \begin{pmatrix} +0.010856 & -0.002401 & +0.999938 \\ -0.002452 & +0.999994 & +0.002428 \\ -0.999938 & -0.002478 & +0.010850 \end{pmatrix}$$

Rotation Angles:

$$\begin{aligned} \text{Angle } (X_c, X_m): \quad & \lambda_{\text{x}} = +89^\circ\ 22'41'' \\ \text{Angle } (Y_c, Y_m): \quad & \mu_{\text{y}} = +0^\circ\ 11'52'' \\ \text{Angle } (Z_c, Z_m): \quad & \nu_{\text{z}} = +89^\circ\ 22'42'' \end{aligned}$$

Determinant of Rotation Matrix: 1.00000
Nominal Field Source: SOLARTRON
Fields applied for 24.0 s
Mean Sensor Temperature: 80.6°C
Automatic Coil Correction: used

Earthfield Compensation: X = DYNAMIC
Y = DYNAMIC
Z = DYNAMIC

Offset Treatment:

A polynomial offset trend of order 2 has been fitted and subtracted from the raw data before creating the sensor model.

Mean Coil System Residual + Sensor Offset: $\underline{B}^{or} = (31.654\ ,\ 12.778\ ,\ 7.066)$ nT

Raw Data Quality:

Standard Deviation of used Raw Data Blocks:

[Values in eng nT]	s_x	s_y	s_z
Minimum	0.011	0.015	0.015
Mean	0.051	0.043	0.060
Maximum	0.126	0.112	0.363

Calibration Parameter:

$$\text{Transfermatrix:} \quad \underline{\underline{\phi}} = \underline{\underline{R}}_{\text{nom}} \underline{\underline{\rho}} \, \underline{\underline{\omega}} \, \underline{\underline{\sigma}} = \begin{pmatrix} +0.997483 & +0.002452 & -0.010822 \\ -0.008020 & +0.998411 & +0.002421 \\ +0.005754 & -0.000411 & +0.997292 \end{pmatrix}$$

$$\text{Reduced Transfermatrix:} \quad \underline{\underline{\tilde{\phi}}} = \underline{\underline{\omega}} \, \underline{\underline{\sigma}} = \begin{pmatrix} +0.997503 & +0.000000 & +0.000000 \\ -0.005562 & +0.998412 & +0.000000 \\ -0.005088 & +0.001987 & +0.997353 \end{pmatrix}$$

$$\text{Sensitivity:} \quad \underline{\underline{\sigma}} = \begin{pmatrix} +0.997503 & +0.000000 & +0.000000 \\ +0.000000 & +0.998396 & +0.000000 \\ +0.000000 & +0.000000 & +0.997338 \end{pmatrix}$$

$$\text{Misalignment:} \quad \underline{\underline{\omega}} = \begin{pmatrix} +1.000000 & +0.000000 & +0.000000 \\ -0.005576 & +1.000016 & +0.000000 \\ -0.005101 & +0.001990 & +1.000015 \end{pmatrix}$$

Sensor Misalignment Angles:

$$\xi_{\text{x,y}} = +89^\circ\ 40'50''$$
$$\xi_{\text{x,z}} = +89^\circ\ 42'30''$$
$$\xi_{\text{y,z}} = +90^\circ\ 6'45''$$

Model Quality:

Standard Deviation, Maximum and Minimum Error of Calculated Model:

[Values in nT]	X	Y	Z
Standard Deviation	0.684	0.215	2.259
Maximum Error	0.981	0.408	3.520
Minimum Error	-1.412	-0.453	-4.981

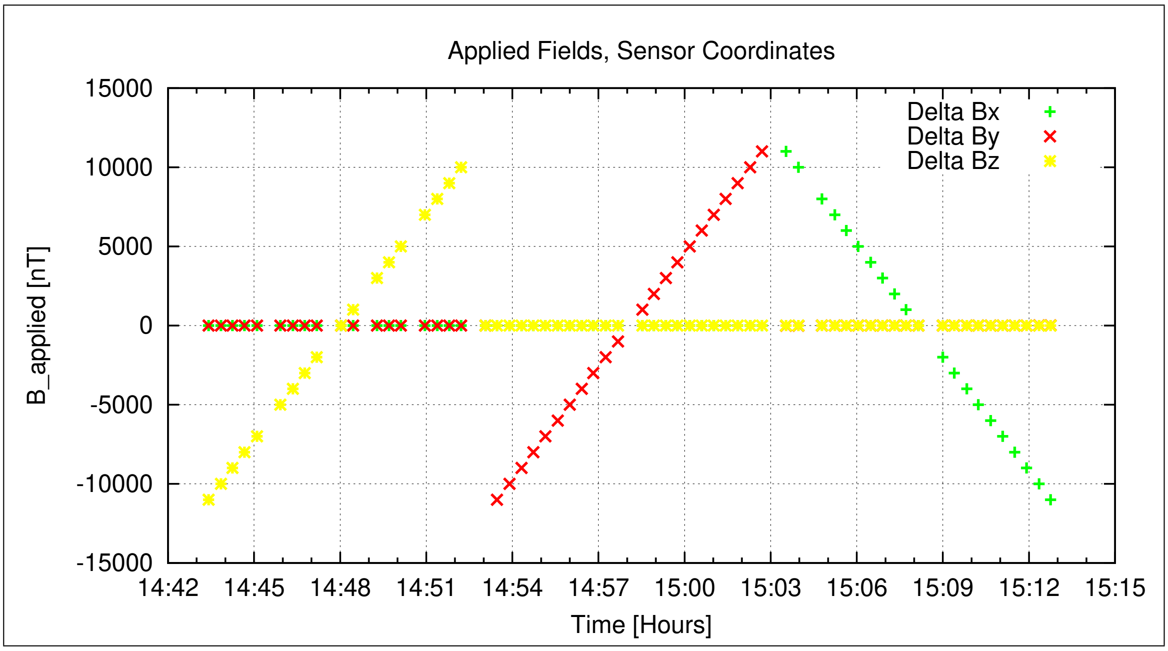

Figure 18: Applied Fields

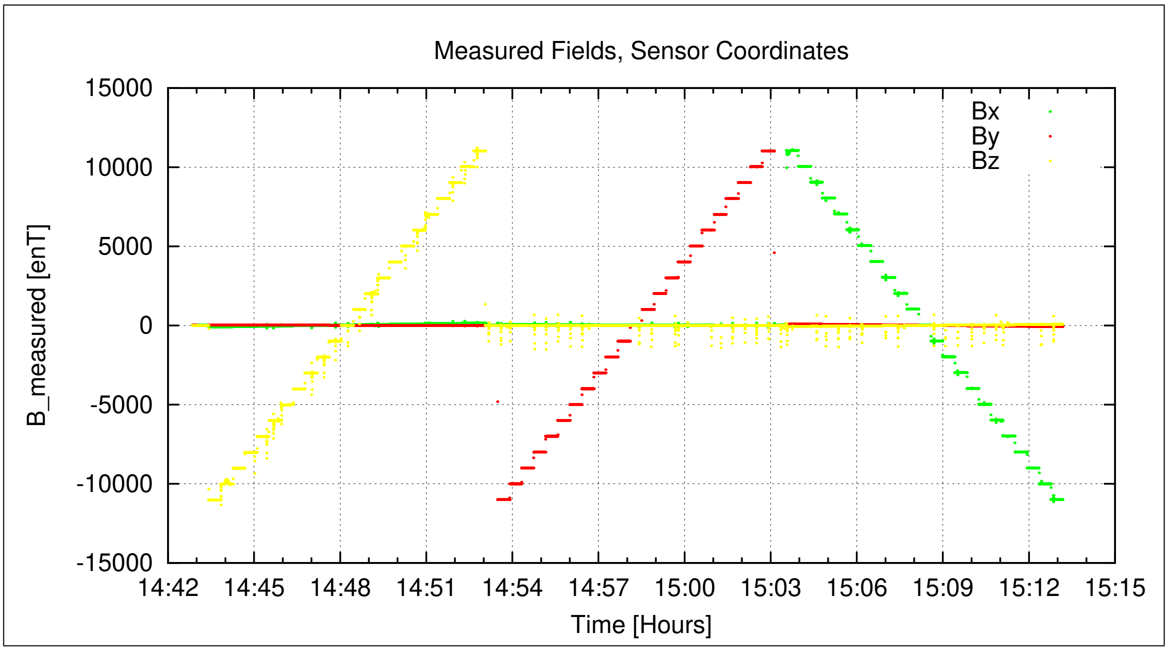

Figure 19: Measured Data

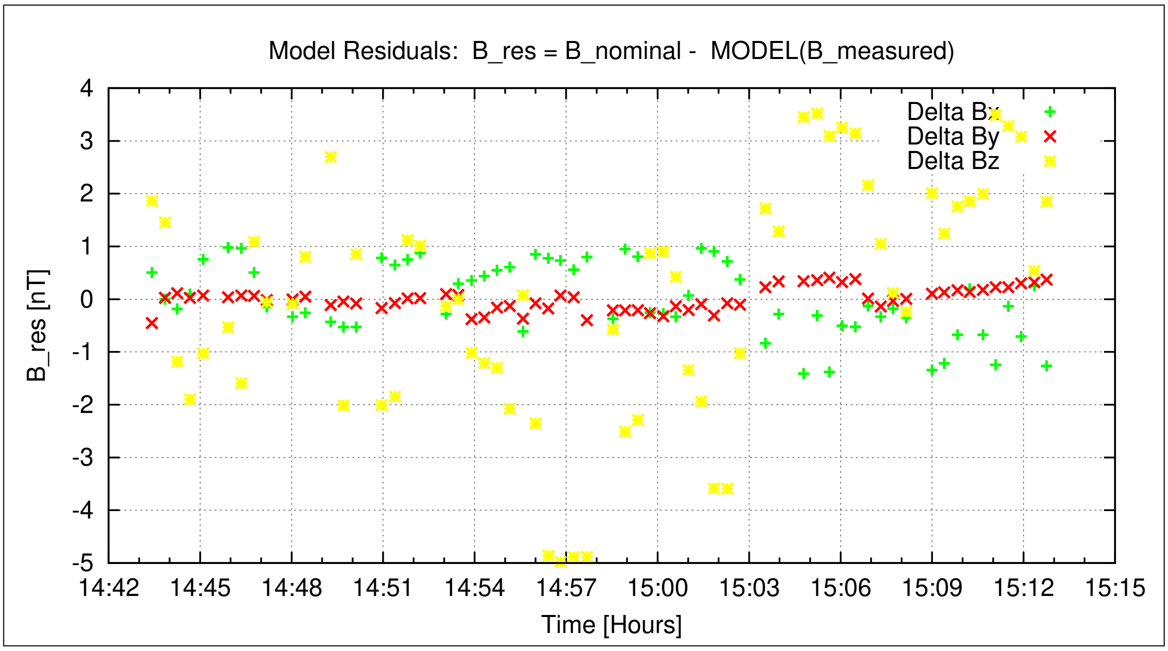

Figure 20: Model Quality - Differences of applied field and modelled measurement data

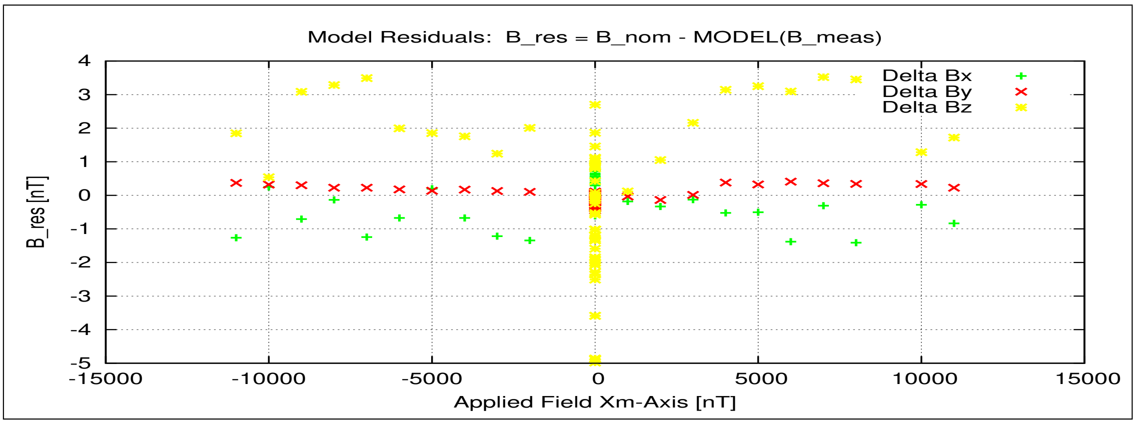

Figure 21: RESIDUALS vs FLD X

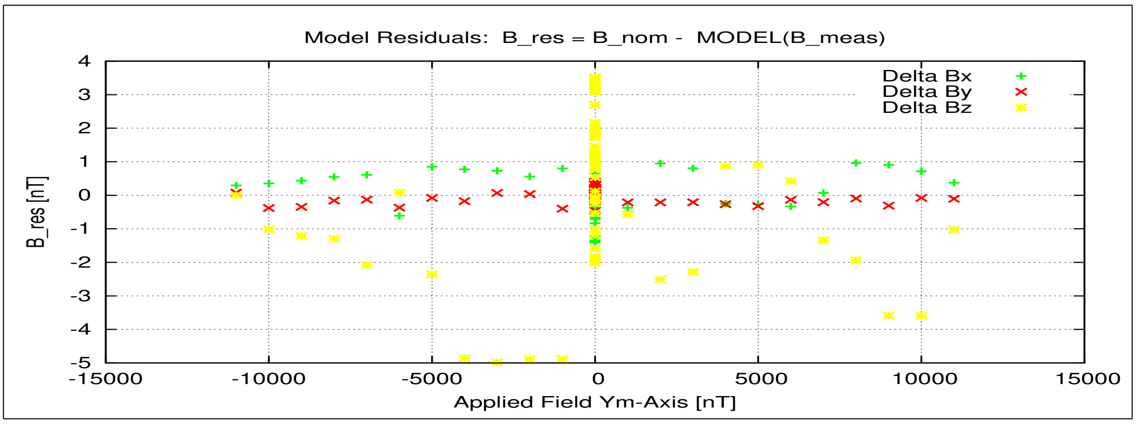

Figure 22: RESIDUALS vs FLD Y

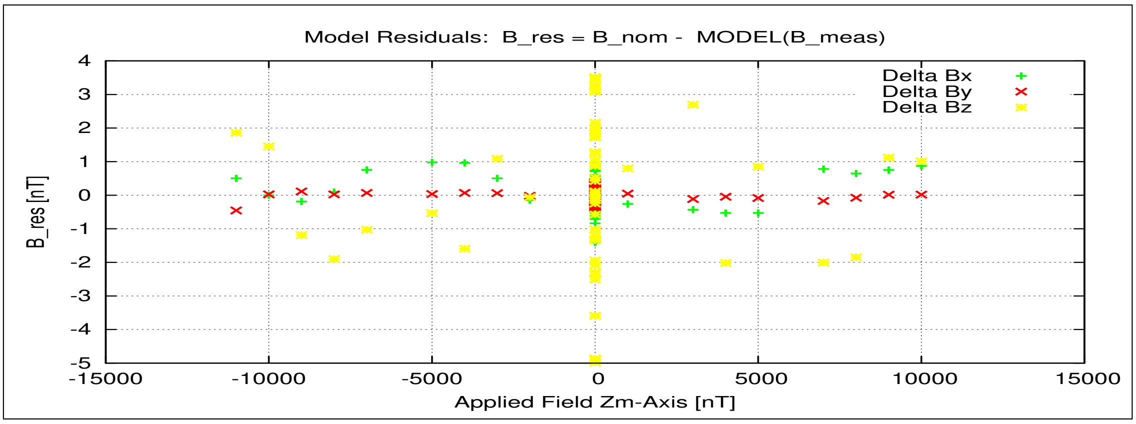

Figure 23: RESIDUALS vs FLD Z

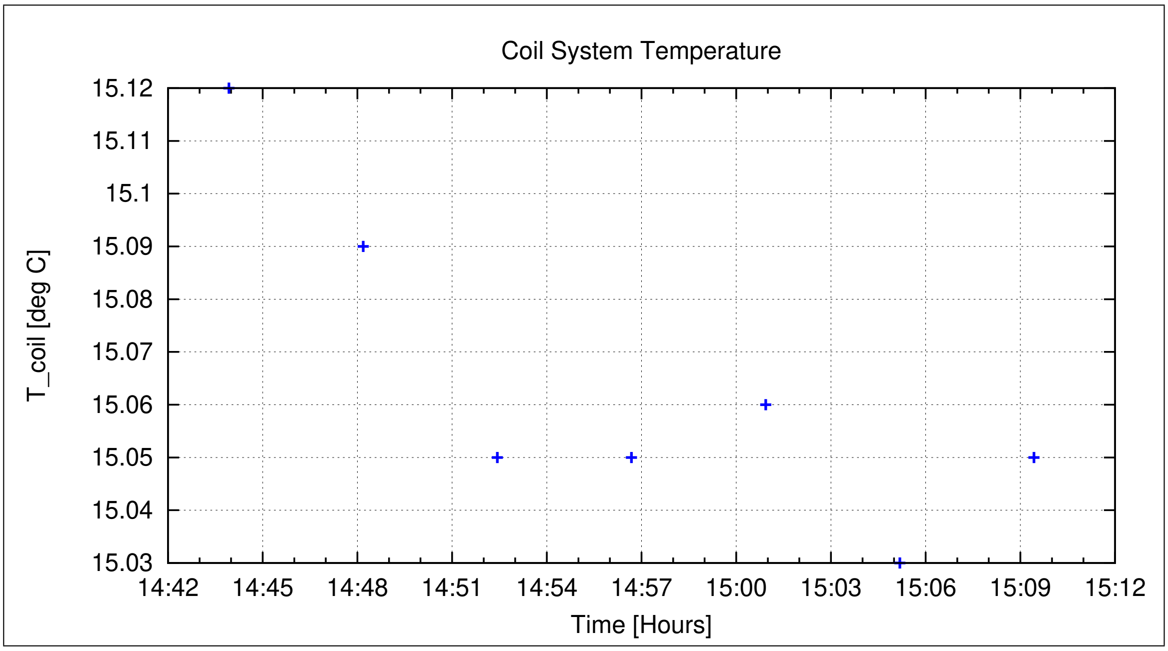

Figure 24: Coil System Temperature

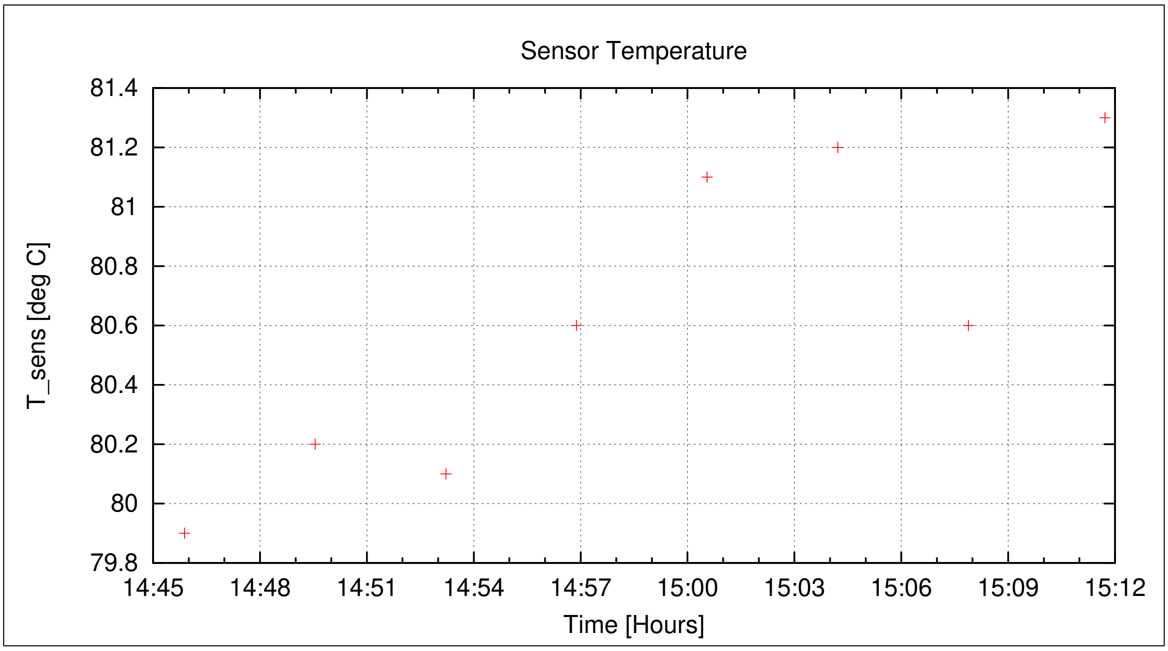

Figure 25: Sensor Temperature

Thermal Analysis: refer to section 8.

6.8 AC-Analysis at Very High Temperature

A frequency measurement was performed at 80°C.

Thermal Analysis: refer to section 8.

Afterwards the heating system was switched off for smooth cooling down to room temperature.

6.9 DC-Analysis at Very High Temperature

Linearity and offset measurements were performed at $T_{59} = +80°C$.

Thermal Analysis: refer to section 8.

Linearity measurements and zerofield measurements in fixed compensated earthfield conditions were conducted during the night.

7 Measurements on January 15, 2014

07:20 inspection of the system. It showed up that the EGSE has crashed again at about 17:10 last evening. Besides that everything was ok. The linearity measurement was stopped. The system was at a temperature of $T_{59} = +40°$.

7.1 Data

CCD File	Configuration File	Remark
14-01-15\07-52-01.CCR	NULL.MAG	
14-01-15\08-34-41.CCR	LIN11000XYZ.MAG	
14-01-15\08-36-01.CCR	LIN11000XYZ.MAG	
14-01-15\08-38-30.CCR	LIN11000XYZ.MAG	
14-01-15\09-09-01.CCR	LIN11000XYZ.MAG	
14-01-15\09-42-36.CCR	FREQ10000.MAG	
14-01-15\10-26-15.CCR	LIN11000XYZ.MAG	
14-01-15\11-08-47.CCR	OFFSET_200.MAG	

Some test without the MRode CDRS were conducted by David. At 08:21:13 and at 8:25:05 some test were conducted with AC fields of 0.1 Hz and amplitudes of 20000 nT_{pp}, 40000 nT_{pp},32000 nT_{pp}, 30000 nT_{pp} ,and 25000 nT_{pp}.

Afterwards the cooling system was engaged in order to cool the sensor down to +20°C.

7.2 DC-Analysis at Room Temperature with Different Phase Values

A Linearity measurement was performed at $T_{59} = +21°C$. For this measurement the following phase values were used:

- DUT parameters:
  Phase X: 104
  Phase Y: 107
  Phase Z: 109

7.2.1 Calibration on 3 Linear Axes

Used Files:

CCD File	Configuration File	Remark
14-01-15\09-09-01.CCR	LIN11000XYZ.MAG	

Parameter File: PARAMETER_LIN__14-01-15_09-09-01.CPF

Facility Parameter:

Nominal Sensor Setup $\underline{B}_{\text{DUT}} = \underline{\underline{R}}_{\text{nom}} \underline{B}_{\text{c}}$

$$\underline{\underline{R}}_{\text{nom}} = \begin{pmatrix} +1.000000 & +0.000000 & +0.000000 \\ +0.000000 & +1.000000 & +0.000000 \\ +0.000000 & +0.000000 & +1.000000 \end{pmatrix}$$

Calculated Sensor Rotation:

$$\underline{\underline{\rho}} = \begin{pmatrix} +0.999688 & +0.010041 & +0.022871 \\ -0.009948 & +0.999942 & -0.004166 \\ -0.022912 & +0.003937 & +0.999730 \end{pmatrix}$$

Rotation Angles:

$$\begin{aligned} \text{Angle } (X_c, X_m): \quad & \lambda_{\text{x}} = & +1^\circ\ 25'53'' \\ \text{Angle } (Y_c, Y_m): \quad & \mu_{\text{y}} = & +0^\circ\ 37'5'' \\ \text{Angle } (Z_c, Z_m): \quad & \nu_{\text{z}} = & +1^\circ\ 19'56'' \end{aligned}$$

Determinant of Rotation Matrix: 1.00000
Nominal Field Source: SOLARTRON
Fields applied for 23.0 s
Mean Sensor Temperature: 20.1°C
Automatic Coil Correction: used

Earthfield Compensation:	X	=	DYNAMIC
	Y	=	DYNAMIC
	Z	=	DYNAMIC

Offset Treatment:

A polynomial offset trend of order 2 has been fitted and subtracted from the raw data before creating the sensor model.

Mean Coil System Residual + Sensor Offset: $\underline{B}^{or}$ = (20.808 , 12.374 , -5.565) nT

Raw Data Quality:

Standard Deviation of used Raw Data Blocks:

[Values in eng nT]	s_x	s_y	s_z
Minimum	0.016	0.008	0.013
Mean	0.058	0.041	0.052
Maximum	0.139	0.109	0.156

Calibration Parameter:

$$\text{Transfermatrix:} \quad \underline{\underline{\phi}} = \underline{\underline{R}}_{\text{nom}} \underline{\underline{\rho}} \, \underline{\underline{\omega}} \, \underline{\underline{\sigma}} = \begin{pmatrix} +0.997896 & +0.010082 & +0.022843 \\ -0.015353 & +0.999026 & -0.004160 \\ -0.027829 & +0.006138 & +0.998496 \end{pmatrix}$$

$$\text{Reduced Transfermatrix:} \quad \widetilde{\underline{\underline{\phi}}} = \underline{\underline{\omega}} \, \underline{\underline{\sigma}} = \begin{pmatrix} +0.998375 & +0.000000 & +0.000000 \\ -0.005442 & +0.999093 & +0.000000 \\ -0.004935 & +0.002205 & +0.998766 \end{pmatrix}$$

$$\text{Sensitivity:} \quad \underline{\underline{\sigma}} = \begin{pmatrix} +0.998375 & +0.000000 & +0.000000 \\ +0.000000 & +0.999078 & +0.000000 \\ +0.000000 & +0.000000 & +0.998752 \end{pmatrix}$$

$$\text{Misalignment:} \quad \underline{\underline{\omega}} = \begin{pmatrix} +1.000000 & +0.000000 & +0.000000 \\ -0.005450 & +1.000015 & +0.000000 \\ -0.004943 & +0.002207 & +1.000015 \end{pmatrix}$$

Sensor Misalignment Angles:

$$\begin{aligned} \xi_{\text{x,y}} &= +89^\circ\ 41'16'' \\ \xi_{\text{x,z}} &= +89^\circ\ 43'3'' \\ \xi_{\text{y,z}} &= +90^\circ\ 7'30'' \end{aligned}$$

Model Quality:

Standard Deviation, Maximum and Minimum Error of Calculated Model:

[Values in nT]	X	Y	Z
Standard Deviation	0.360	0.181	1.571
Maximum Error	1.725	0.680	3.125
Minimum Error	-0.883	-0.286	-3.441

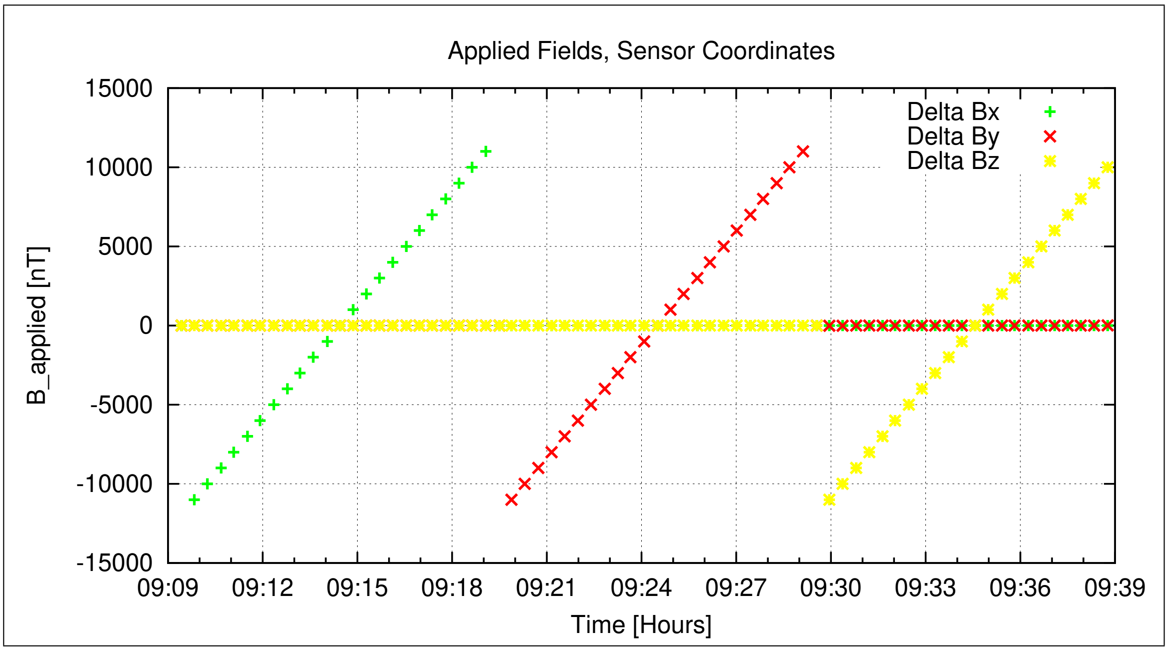

Figure 26: Applied Fields

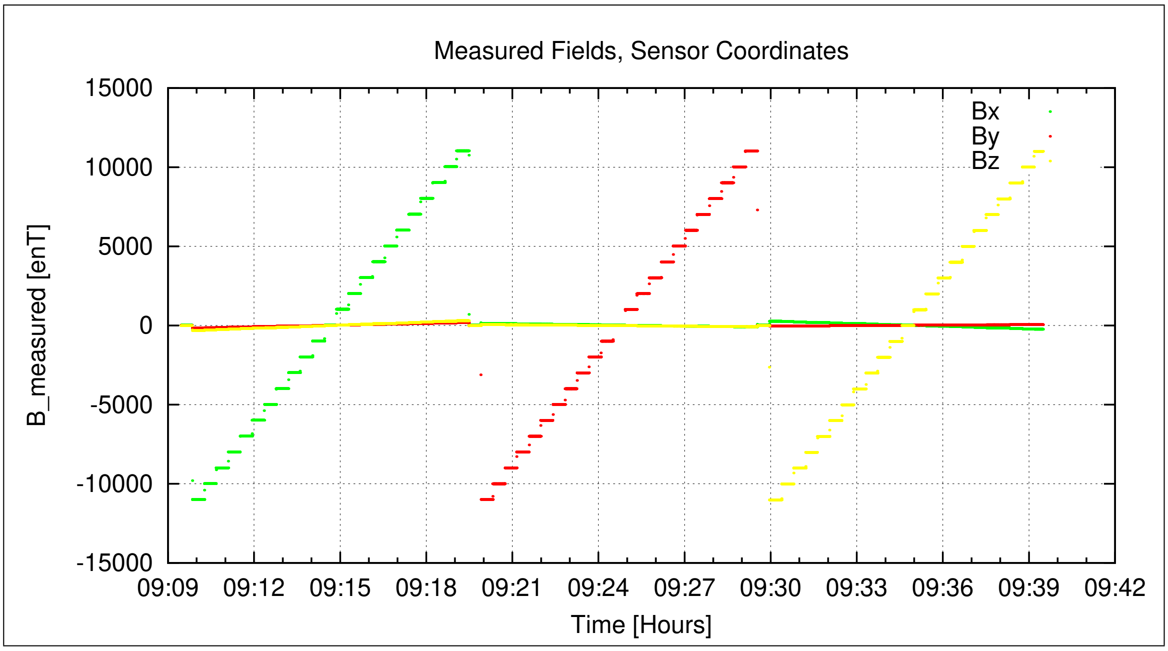

Figure 27: Measured Data

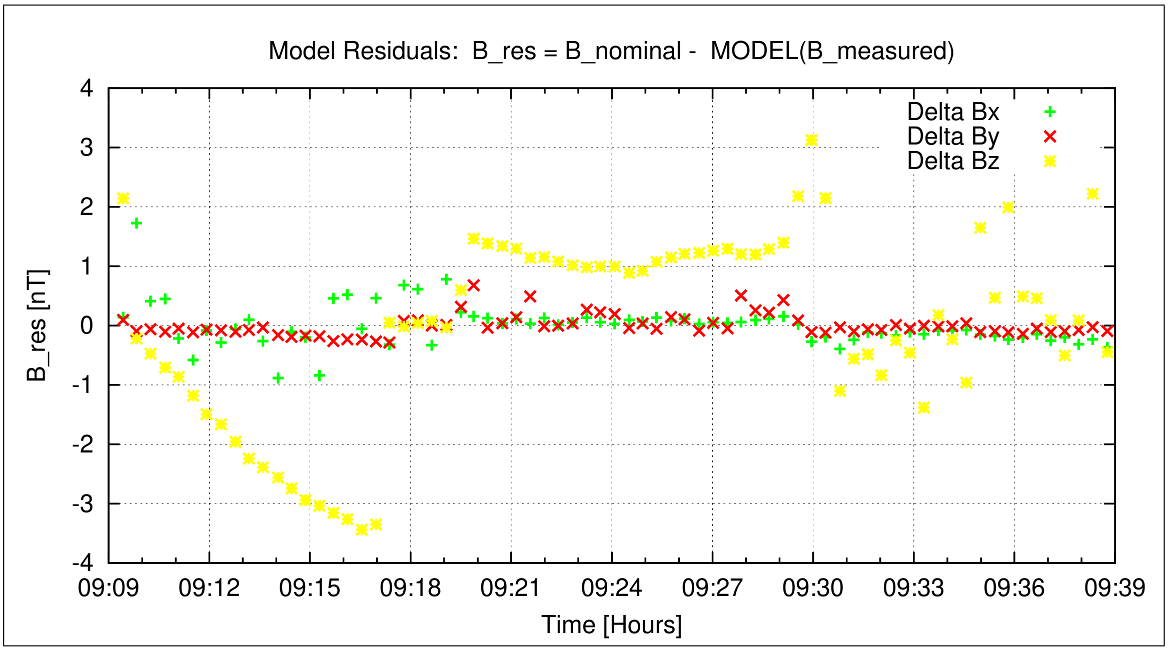

Figure 28: Model Quality - Differences of applied field and modelled measurement data

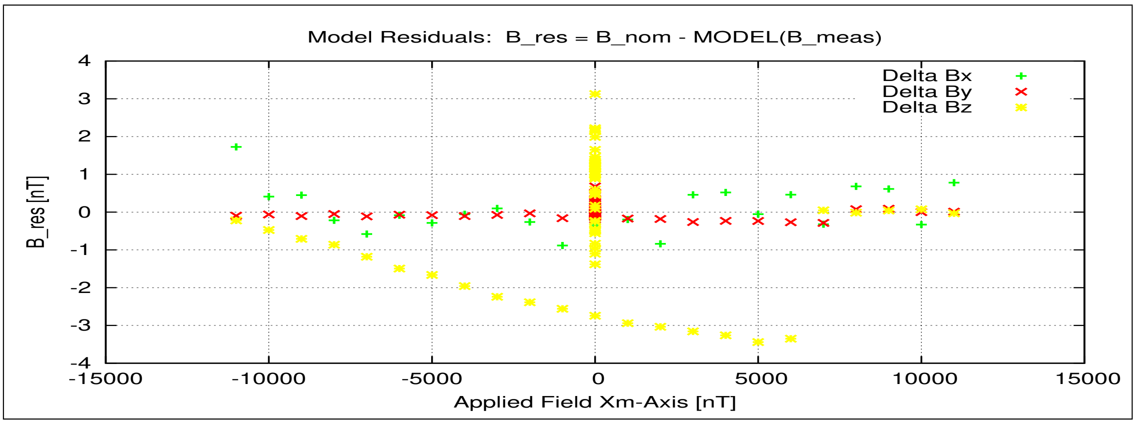

Figure 29: RESIDUALS vs FLD X

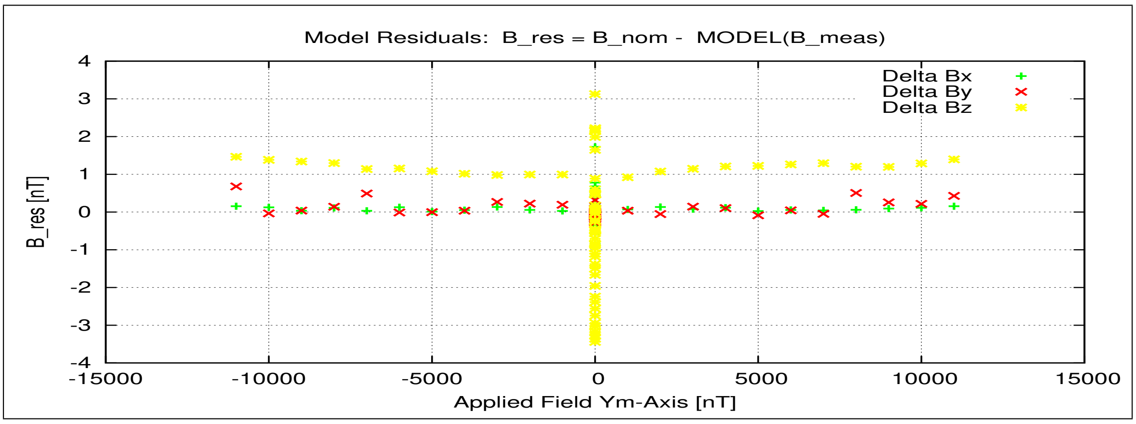

Figure 30: RESIDUALS vs FLD Y

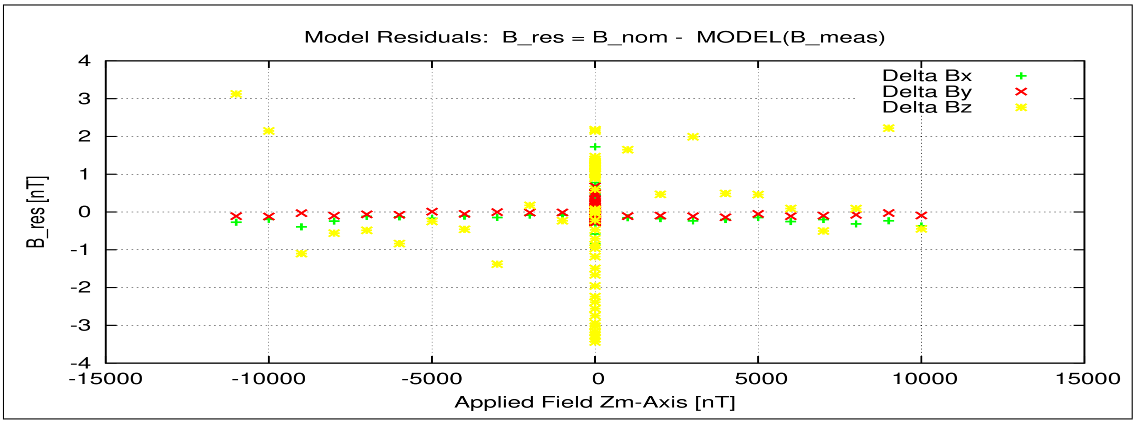

Figure 31: RESIDUALS vs FLD Z

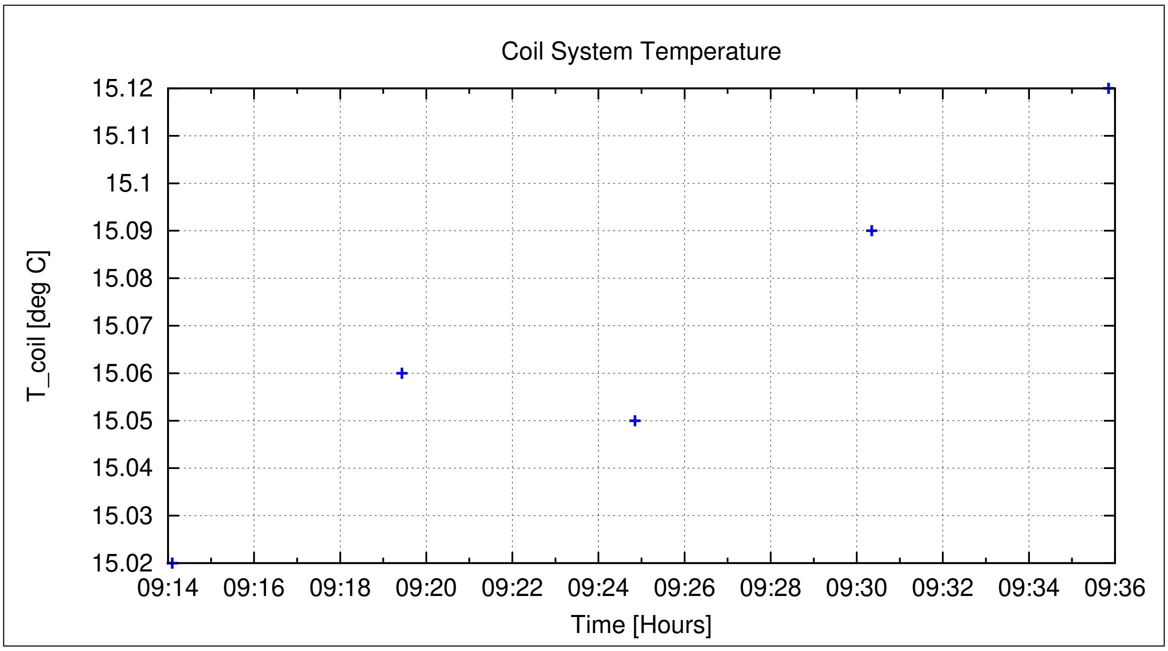

Figure 32: Coil System Temperature

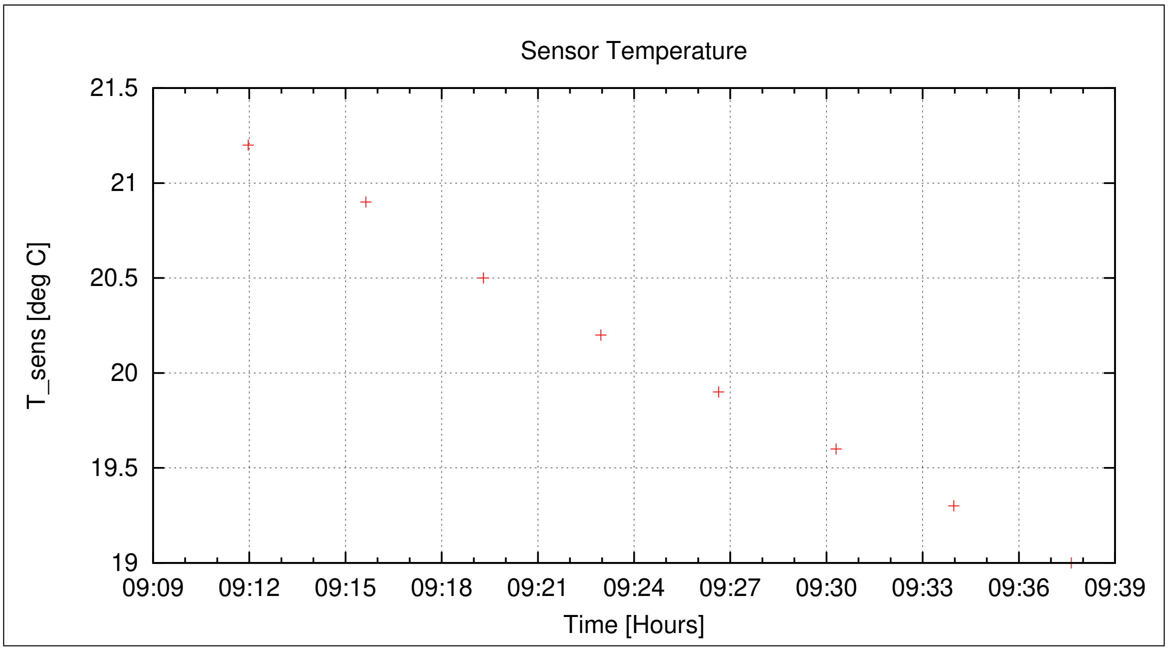

Figure 33: Sensor Temperature

After the measurement the phase values were set back to the default values.

Thermal Analysis: refer to section 8.

7.3 AC-Analysis at Room Temperature

A frequency measurement was performed at 20°C.

Setup:

- Sensor mounted in thermal box. CoC. Box vertical.
- Sensor rotated to:
  Elevation= 45°
  Azimuth= 126°
- Field applied on Y_c.
- No attenuator

7.3.1 Frequency Measurements

This section is dedicated to the frequency behavior of the instrument. The analysis of the performed AC measurements allows to calculate the actual sampling frequency f_s of the instrument and the frequency response (amplitude vs. frequency). The measurements have been performed with the sensor placed at CoC in a diagonal in space orientation. The AC-fields have been applied on the Y_c axis only. Using this setup it can be guaranteed that only one frequency is applied at a time and no beat effects occur.

Used Frequency Measurements:

CCD File	Configuration File	Remark
`14-01-15\09-42-36.CCR`	`FREQ10000.MAG`	

Parameter File: `FREQ_PARAMETER__14-01-15-09-42-36.FPF`

Calibration Parameter:

Sampling Frequency:

Component	f_s [Hz]	Standard deviation [Hz]
X	10.0000	0.000056
Y	10.0002	0.000539
Z	10.0000	0.000090
Mean Sampling Frequency	10.0001	0.000155

3 dB Corner Frequency:

Component	$f_{3\mathrm{dB}}$ [Hz]
X	5.59
Y	5.58
Z	5.59

Applied Frequencies and Measured Amplitudes

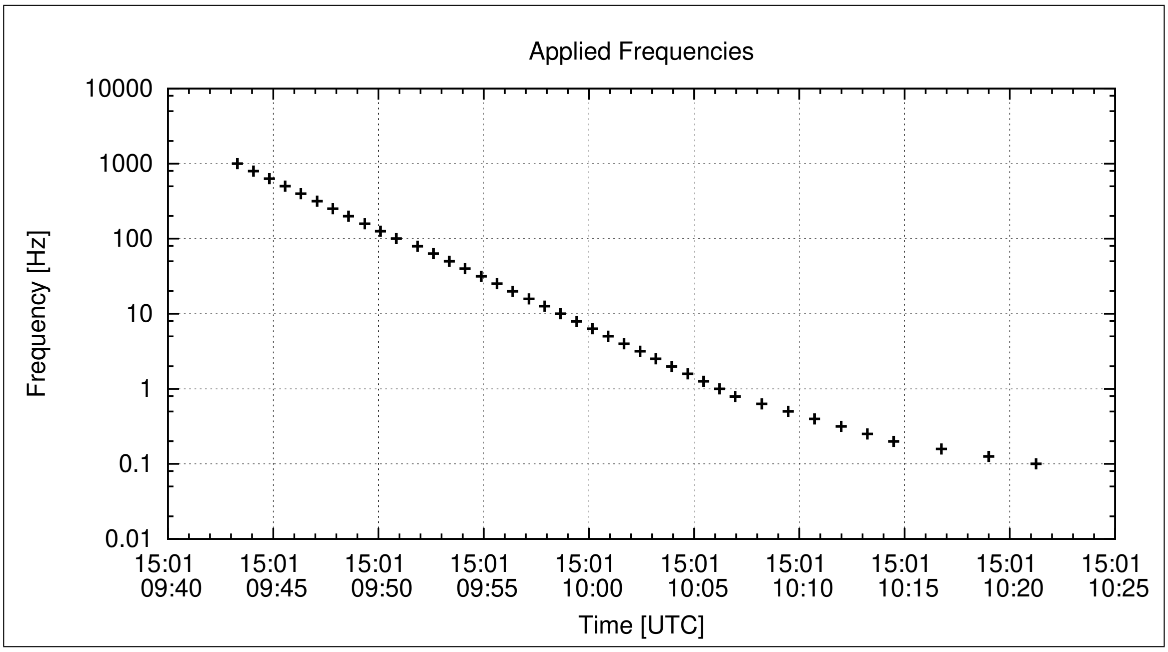

Figure 34: Applied Frequencies for AC Analysis

Applied Frequency [Hz]	Bx [enT]	By [enT]	Bz [enT]
1000.000	43.99	29.05	35.80
794.000	47.63	51.38	36.10
631.000	0.27	0.14	0.08
501.000	122.19	139.67	97.07
398.000	144.06	163.12	119.95
316.000	0.92	0.78	0.79
251.000	10.89	6.27	10.02
199.000	181.14	207.80	156.40
158.000	36.30	21.42	34.66
126.000	58.96	38.71	55.52
100.000	122.40	76.97	109.45
79.400	28.38	19.74	26.35
63.100	131.33	78.64	125.60
50.100	5.60	2.09	5.43
39.800	14.06	8.75	13.81
31.600	135.67	80.93	134.76
25.100	368.90	235.62	359.83
19.900	15.36	17.16	14.74
15.800	607.21	461.26	568.14
12.600	577.32	482.22	535.49
10.000	1.52	1.21	1.43
7.900	765.70	718.00	712.56
6.310	1425.32	1361.01	1329.94
5.010	1954.50	1875.67	1826.90
3.980	2327.30	2244.30	2176.44
3.160	2582.66	2493.82	2416.55
2.510	2752.10	2658.94	2576.01
1.990	2862.45	2766.77	2679.43
1.580	2932.75	2835.21	2745.96
1.260	2977.35	2879.44	2787.31
1.000	3006.92	2907.99	2814.55
0.790	3025.55	2925.94	2832.63
0.631	3036.86	2937.17	2843.34
0.501	3044.31	2944.35	2850.00
0.398	3049.02	2949.10	2855.01
0.316	3051.69	2951.47	2856.99
0.251	3053.19	2952.50	2858.37
0.199	3055.41	2955.16	2860.25
0.158	3056.36	2956.29	2861.21
0.126	3056.74	2956.78	2861.55
0.100	3056.75	2955.50	2861.19

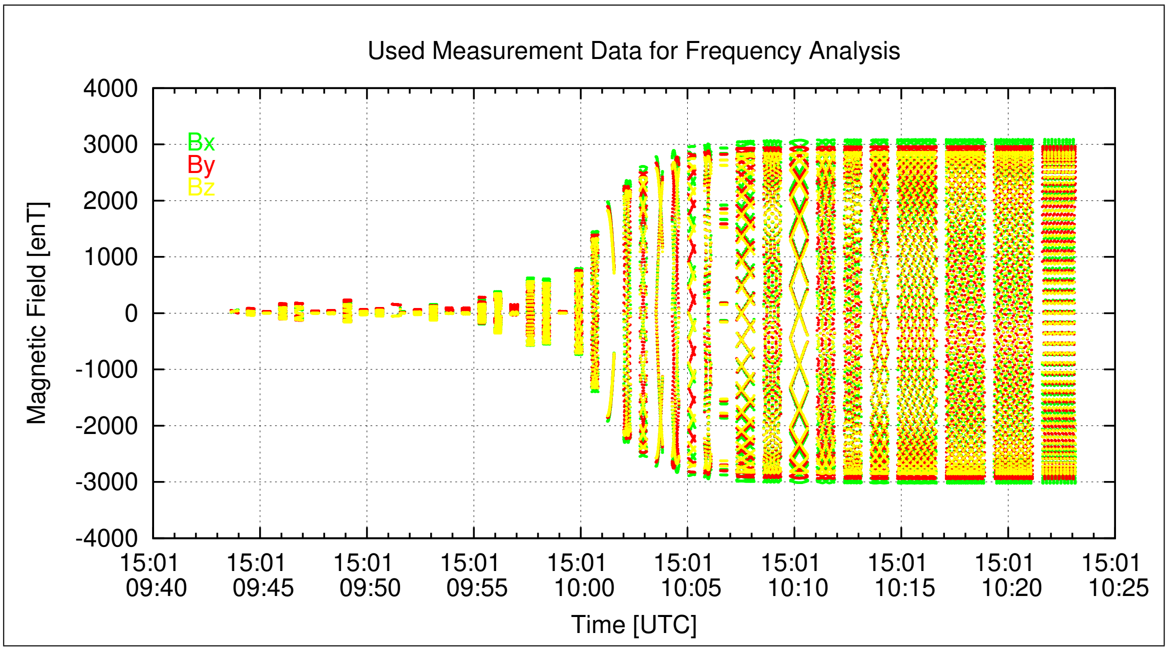

Figure 35: Used packets of Measured data for the Frequency analysis

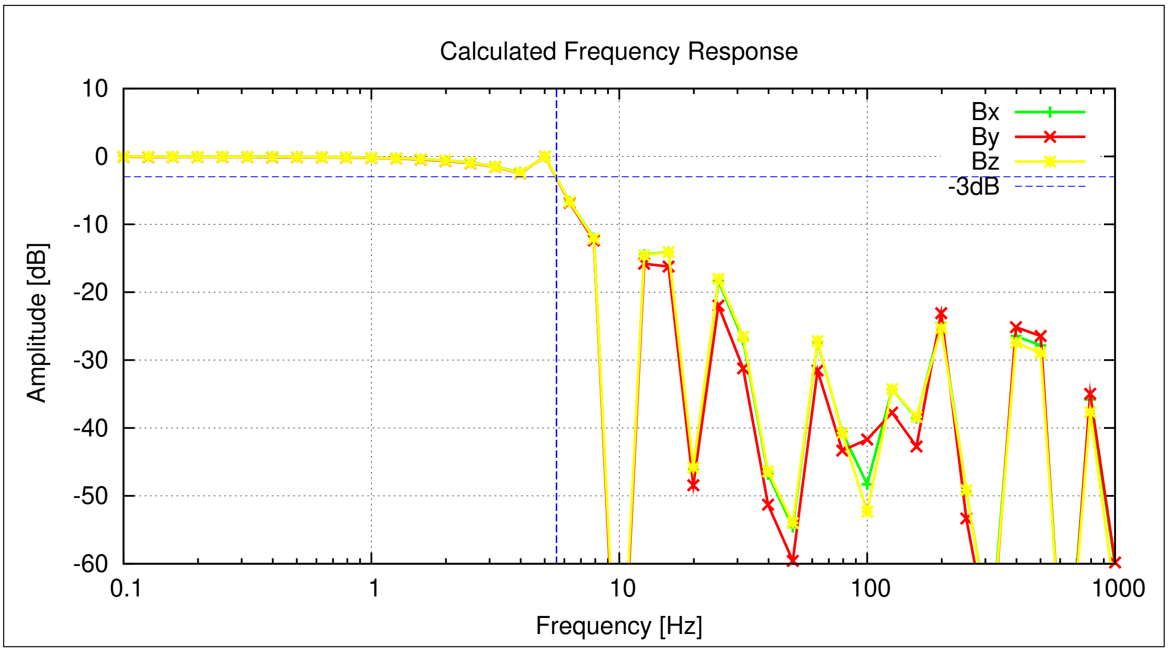

Figure 36: Calculated Frequency Response

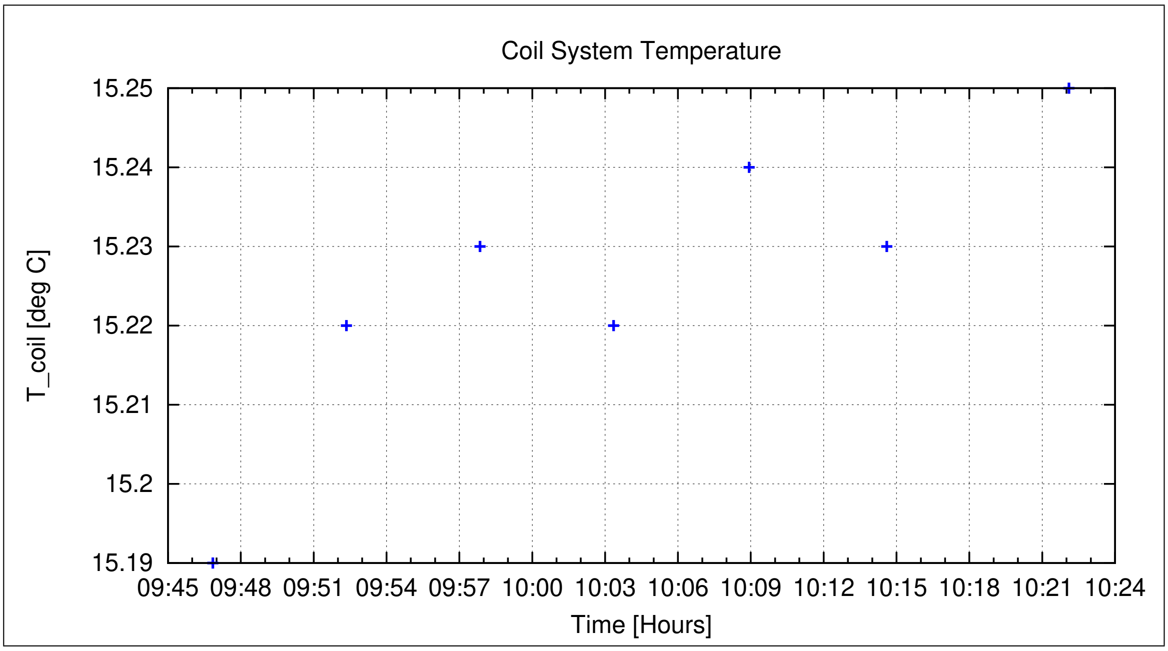

Figure 37: Coil System Temperature

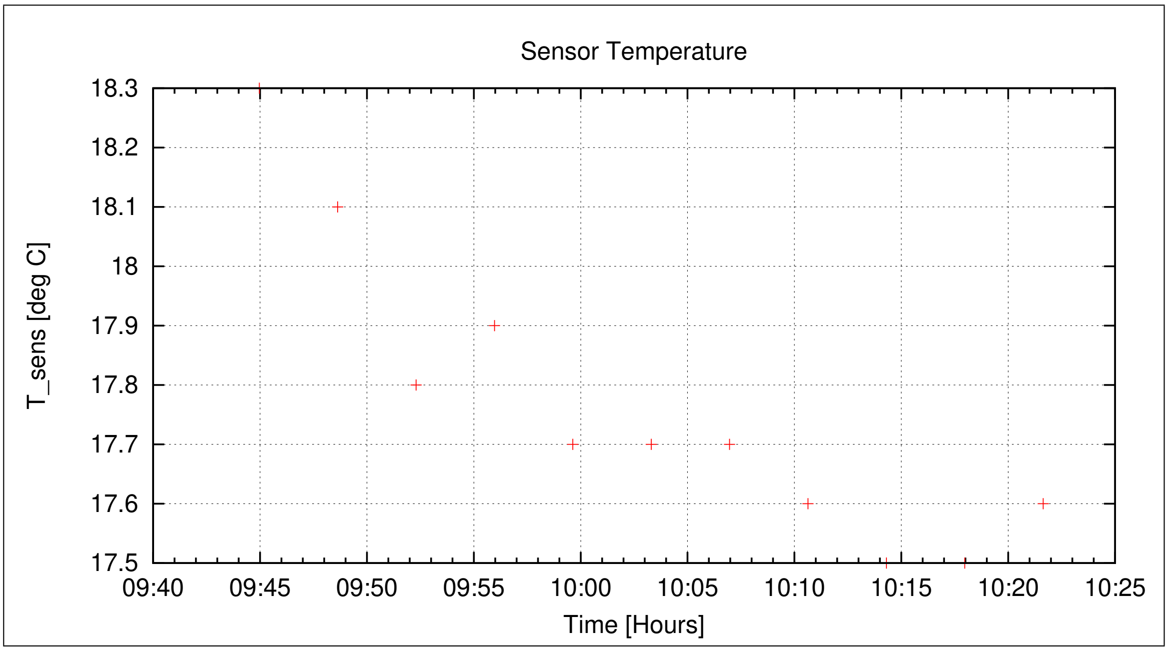

Figure 38: Sensor Temperature

7.4 DC-Analysis at Environmental Temperature

A standard linearity and offset measurement was performed at 17°C.

7.4.1 Calibration on 3 Linear Axes

Used Files:

CCD File	Configuration File	Remark
`14-01-15\10-26-15.CCR`	`LIN11000XYZ.MAG`	

Parameter File: `PARAMETER_LIN__14-01-15_10-26-15.CPF`

Facility Parameter:

Nominal Sensor Setup $\underline{B}_{\mathrm{DUT}} = \underline{\underline{R}}_{\mathrm{nom}} \underline{B}_{\mathrm{c}}$

$$\underline{\underline{R}}_{\mathrm{nom}} = \begin{pmatrix} +1.000000 & +0.000000 & +0.000000 \\ +0.000000 & +1.000000 & +0.000000 \\ +0.000000 & +0.000000 & +1.000000 \end{pmatrix}$$

Calculated Sensor Rotation:

$$\underline{\underline{\rho}} = \begin{pmatrix} +0.999552 & +0.008937 & +0.028582 \\ -0.008807 & +0.999950 & -0.004653 \\ -0.028622 & +0.004399 & +0.999581 \end{pmatrix}$$

Rotation Angles:

$$\begin{aligned} \text{Angle } (X_c, X_m): &\quad \lambda_{\mathrm{x}} = +1^\circ\ 42'58'' \\ \text{Angle } (Y_c, Y_m): &\quad \mu_{\mathrm{y}} = +0^\circ\ 34'15'' \\ \text{Angle } (Z_c, Z_m): &\quad \nu_{\mathrm{z}} = +1^\circ\ 39'34'' \end{aligned}$$

Determinant of Rotation Matrix: 1.00000
Nominal Field Source: SOLARTRON
Fields applied for 23.0 s
Mean Sensor Temperature: 18.0°C
Automatic Coil Correction: used

Earthfield Compensation: X = DYNAMIC
Y = DYNAMIC
Z = DYNAMIC

Offset Treatment:

A polynomial offset trend of order 2 has been fitted and subtracted from the raw data before creating the sensor model.

Mean Coil System Residual + Sensor Offset: $\underline{B}^{or}$ = (20.464 , 11.951 , -4.210) nT

Raw Data Quality:

Standard Deviation of used Raw Data Blocks:

[Values in eng nT]	s_x	s_y	s_z
Minimum	0.004	0.003	0.002
Mean	0.048	0.035	0.040
Maximum	0.128	0.108	0.128

Calibration Parameter:

$$\text{Transfermatrix:}\quad \underline{\underline{\phi}} = \underline{\underline{R}}_{\text{nom}}\,\underline{\underline{\rho}}\,\underline{\underline{\omega}}\,\underline{\underline{\sigma}} = \begin{pmatrix} +0.997808 & +0.008991 & +0.028549 \\ -0.014244 & +0.999066 & -0.004648 \\ -0.033708 & +0.006575 & +0.998420 \end{pmatrix}$$

$$\text{Reduced Transfermatrix:}\quad \tilde{\underline{\underline{\phi}}} = \underline{\underline{\omega}}\,\underline{\underline{\sigma}} = \begin{pmatrix} +0.998451 & +0.000000 & +0.000000 \\ -0.005475 & +0.999126 & +0.000000 \\ -0.005108 & +0.002181 & +0.998839 \end{pmatrix}$$

$$\text{Sensitivity:}\quad \underline{\underline{\sigma}} = \begin{pmatrix} +0.998451 & +0.000000 & +0.000000 \\ +0.000000 & +0.999111 & +0.000000 \\ +0.000000 & +0.000000 & +0.998824 \end{pmatrix}$$

$$\text{Misalignment:}\quad \underline{\underline{\omega}} = \begin{pmatrix} +1.000000 & +0.000000 & +0.000000 \\ -0.005483 & +1.000015 & +0.000000 \\ -0.005116 & +0.002183 & +1.000015 \end{pmatrix}$$

Sensor Misalignment Angles:

$$\begin{aligned} \xi_{\text{x,y}} &= +89^\circ\ 41'9'' \\ \xi_{\text{x,z}} &= +89^\circ\ 42'27'' \\ \xi_{\text{y,z}} &= +90^\circ\ 7'24'' \end{aligned}$$

Model Quality:

Standard Deviation, Maximum and Minimum Error of Calculated Model:

[Values in nT]	X	Y	Z
Standard Deviation	0.416	0.144	0.834
Maximum Error	0.714	0.449	3.379
Minimum Error	-0.902	-0.262	-0.873

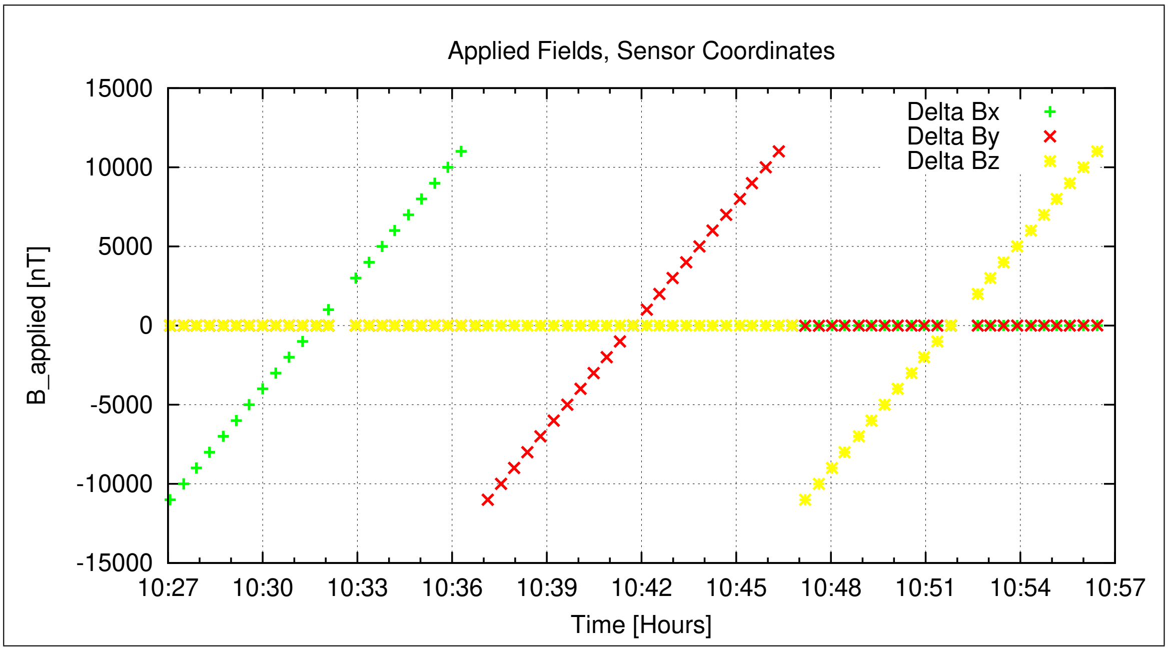

Figure 39: Applied Fields

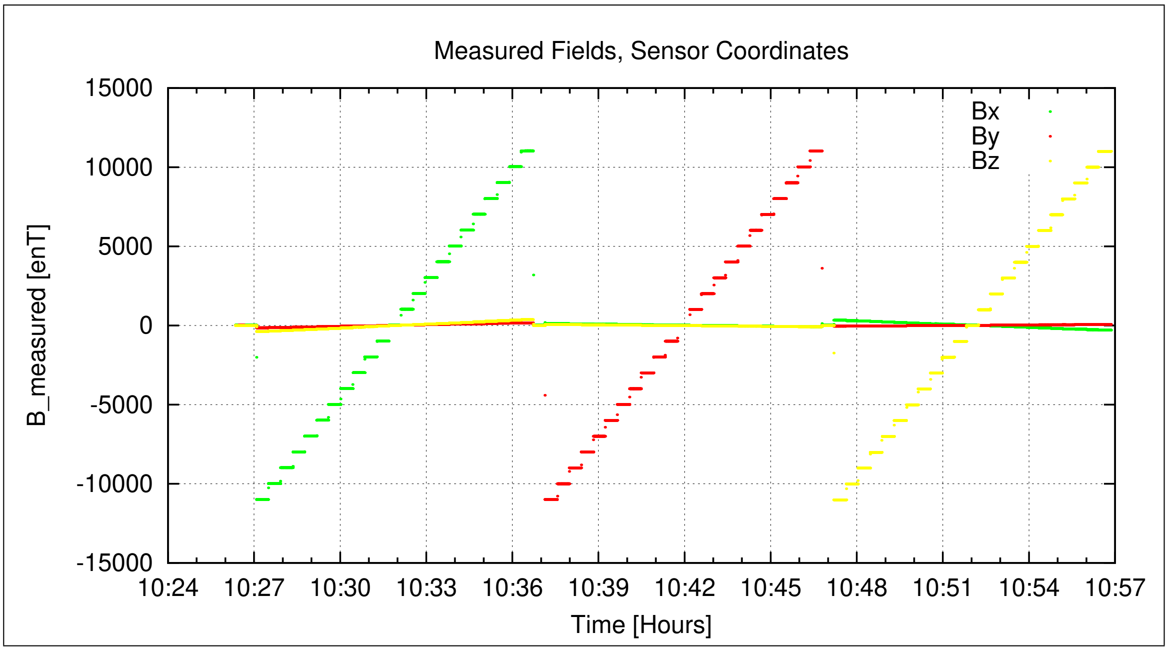

Figure 40: Measured Data

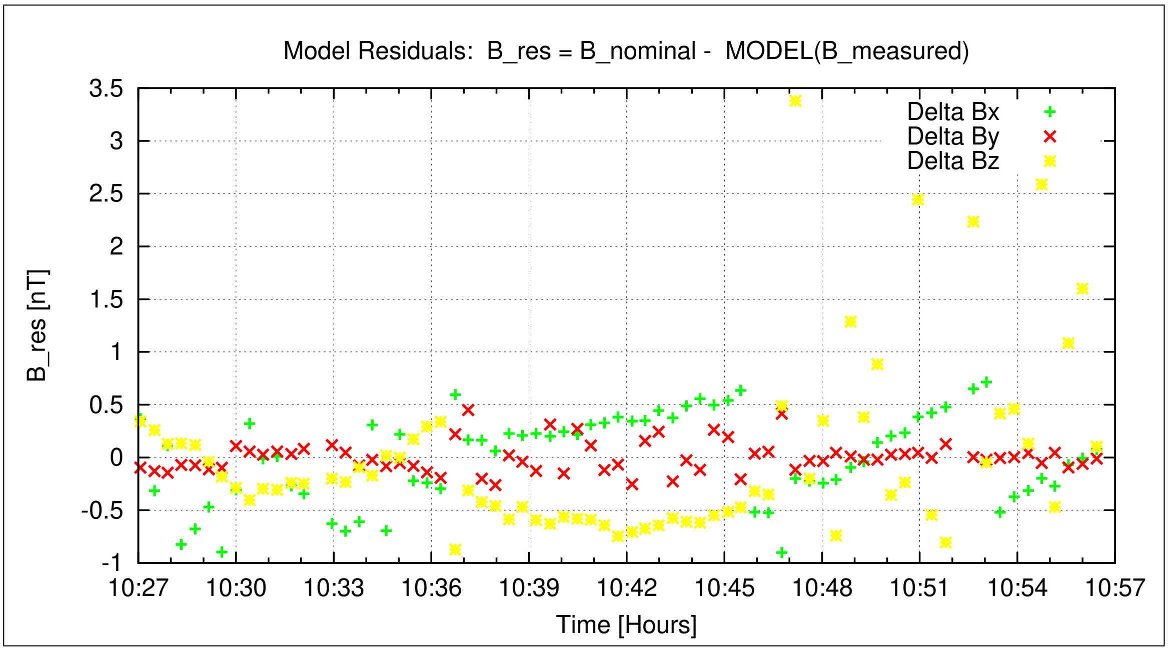

Figure 41: Model Quality - Differences of applied field and modelled measurement data

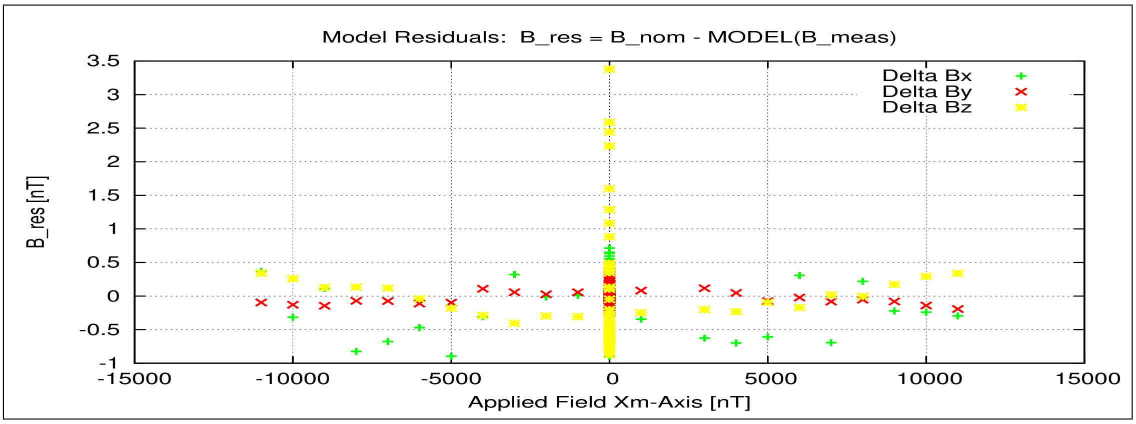

Figure 42: RESIDUALS vs FLD X

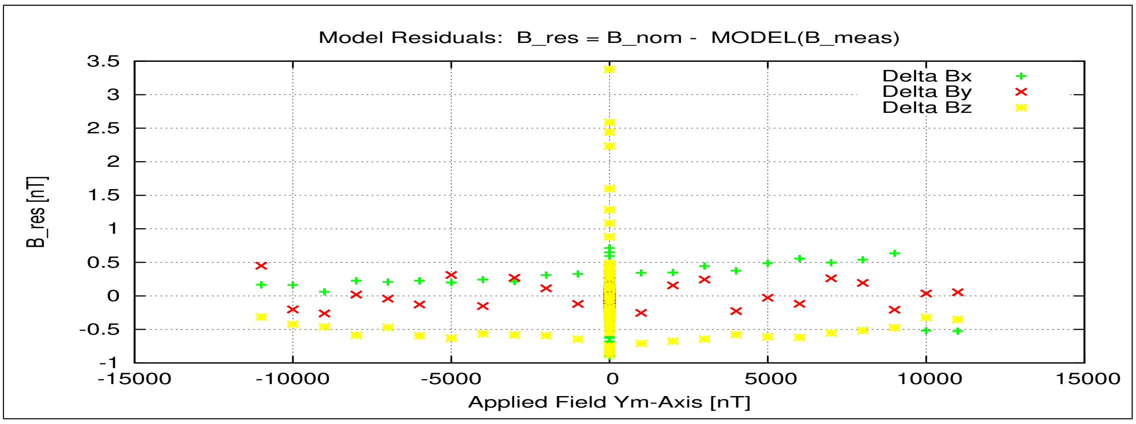

Figure 43: RESIDUALS vs FLD Y

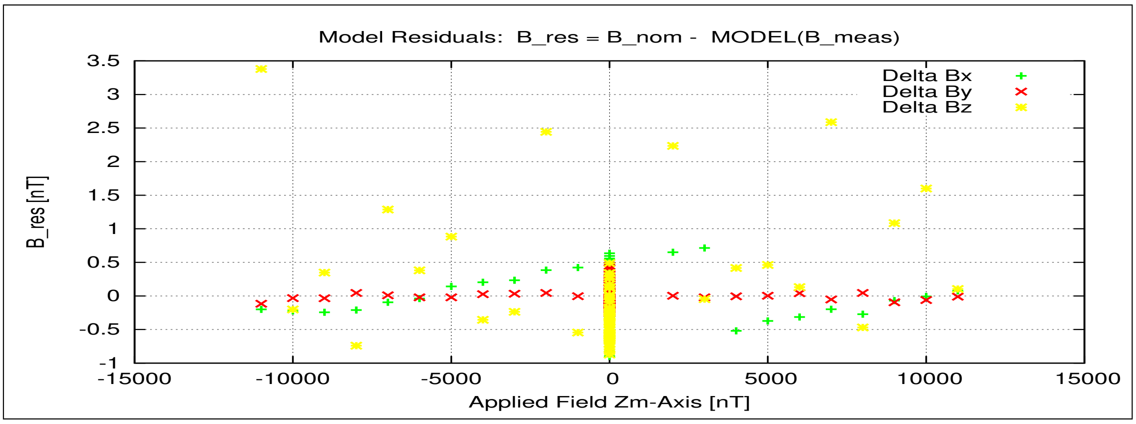

Figure 44: RESIDUALS vs FLD Z

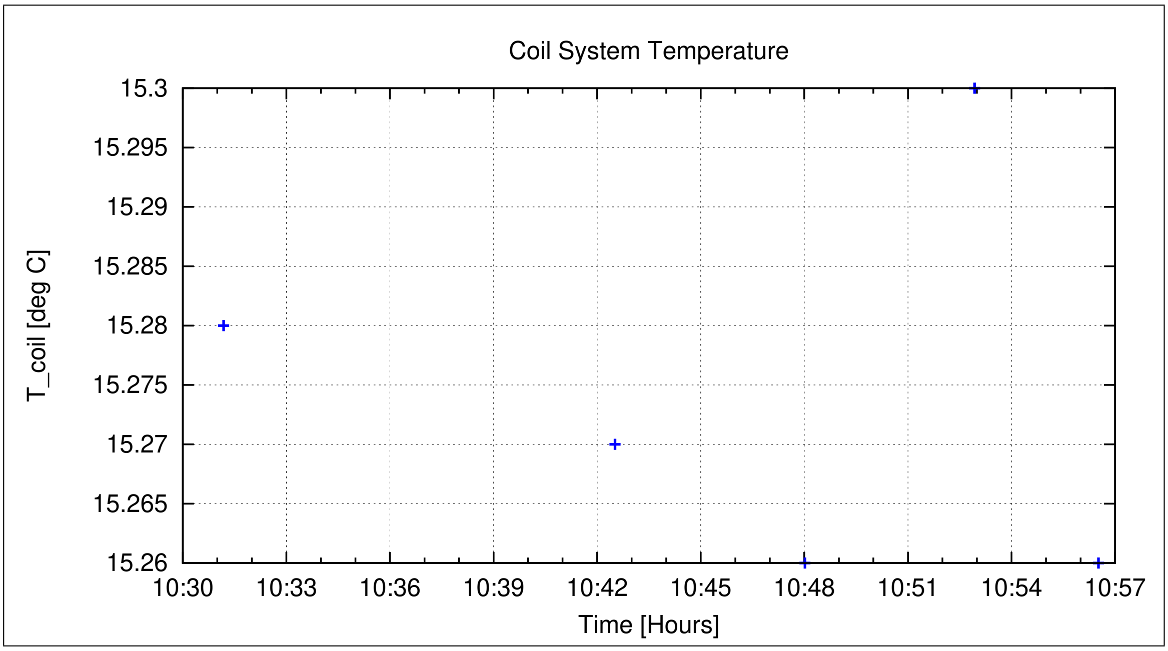

Figure 45: Coil System Temperature

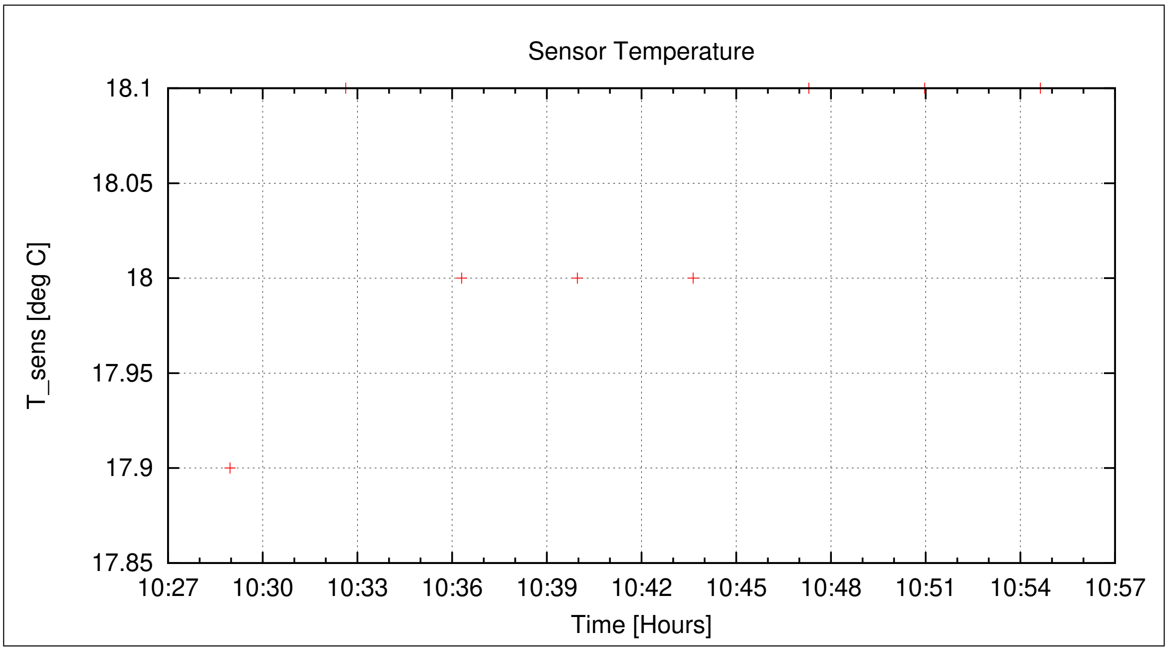

Figure 46: Sensor Temperature

7.4.2 OFFSET Calculation

In this section the instrument offsets and the residual field of the Coil System will be evaluated. Measurements at two orientations for each component act as input for the offset calculation. From the "normal" (0-degrees) and "turned" (180-degrees) orientations the offsets and residual fields can be derived:

$$B_{\text{off}} = \frac{B_{\text{normal}} + B_{\text{turned}}}{2}$$
$$B_{\text{res}} = \frac{B_{\text{normal}} - B_{\text{turned}}}{2}$$

Used Offset Measurements:

CCD File	Configuration File	Remark
14-01-15\11-08-47.CCR	OFFSET_200.MAG	

Parameter File: OFF_PARAMETER__14-01-15-11-08-47.OPF

Calibration Parameter:

Sensor Offsets:

Component	Offset [enT]	Standard deviation [enT]
X	18.63	0.097
Y	13.95	0.120
Z	2.50	0.100

Residual Field of the Coil System:

Component	B_{res} [enT]
X	2.72
Y	-2.44
Z	-1.34

Remark: Residual field is given in actual DUT coordinates, not in coil-coordinates!

The calibration was finished at 11:45.

8 Combined Measurements from January 10 – 15, 2014

8.1 Thermal-Analysis

8.1.1 Temperature Calibration on Linear Axes

Used Temperature Measurements:

Calibration Parameter File	Remark
PARAMETER_TEMPLIN__14-01-10_17-07-01.CPF	
PARAMETER_TEMPLIN__14-01-10_17-37-32.CPF	
PARAMETER_TEMPLIN__14-01-10_21-41-40.CPF	
PARAMETER_TEMPLIN__14-01-13_08-12-34.CPF	
PARAMETER_TEMPLIN__14-01-13_08-52-32.CPF	
PARAMETER_TEMPLIN__14-01-13_09-23-03.CPF	
PARAMETER_TEMPLIN__14-01-13_09-53-35.CPF	
PARAMETER_TEMPLIN__14-01-13_13-05-30.CPF	
PARAMETER_TEMPLIN__14-01-13_13-36-00.CPF	
PARAMETER_TEMPLIN__14-01-13_15-41-19.CPF	
PARAMETER_TEMPLIN__14-01-13_20-46-24.CPF	
PARAMETER_TEMPLIN__14-01-14_00-19-59.CPF	
PARAMETER_TEMPLIN__14-01-14_06-56-35.CPF	
PARAMETER_TEMPLIN__14-01-14_12-19-09.CPF	
PARAMETER_TEMPLIN__14-01-14_12-49-39.CPF	
PARAMETER_TEMPLIN__14-01-14_14-42-36.CPF	
PARAMETER_TEMPLIN__14-01-14_15-13-07.CPF	
PARAMETER_TEMPLIN__14-01-15_09-09-01.CPF	
PARAMETER_TEMPLIN__14-01-15_10-26-15.CPF	

Thermal Parameter File: THERMAL_PARAMETER__14-01-10-17-07-01.TPF

Facility Parameter:

Nominal Sensor Setup $\underline{B}_{\mathrm{DUT}} = \underline{\underline{R}}_{\mathrm{nom}} \underline{B}_{\mathrm{C}}$

$$\underline{\underline{R}}_{\mathrm{nom}} = \begin{pmatrix} +1.000000 & +0.000000 & +0.000000 \\ +0.000000 & +1.000000 & +0.000000 \\ +0.000000 & +0.000000 & +1.000000 \end{pmatrix}$$

Calculated Initial Sensor Rotation:

$$\underline{\underline{R}} = \begin{pmatrix} +0.999545 & +0.008266 & +0.029000 \\ -0.008118 & +0.999953 & -0.005231 \\ -0.029042 & +0.004994 & +0.999566 \end{pmatrix}$$

Initial Rotation Angles:

$$\begin{aligned} \text{Rotation @ X:} \quad \lambda_{\mathrm{x}} &= +1^\circ\ 43'41'' \\ \text{Rotation @ Y:} \quad \mu_{\mathrm{y}} &= +0^\circ\ 33'12'' \\ \text{Rotation @ Z:} \quad \nu_{\mathrm{z}} &= +1^\circ\ 41'19'' \end{aligned}$$

Determinant of Rotation Matrix: 1.0000

Nominal Field Source: SOLARTRON

Automatic Coil correction: used

Used Sensor-Temperature-Channel: T_{59}

Temperature Profile

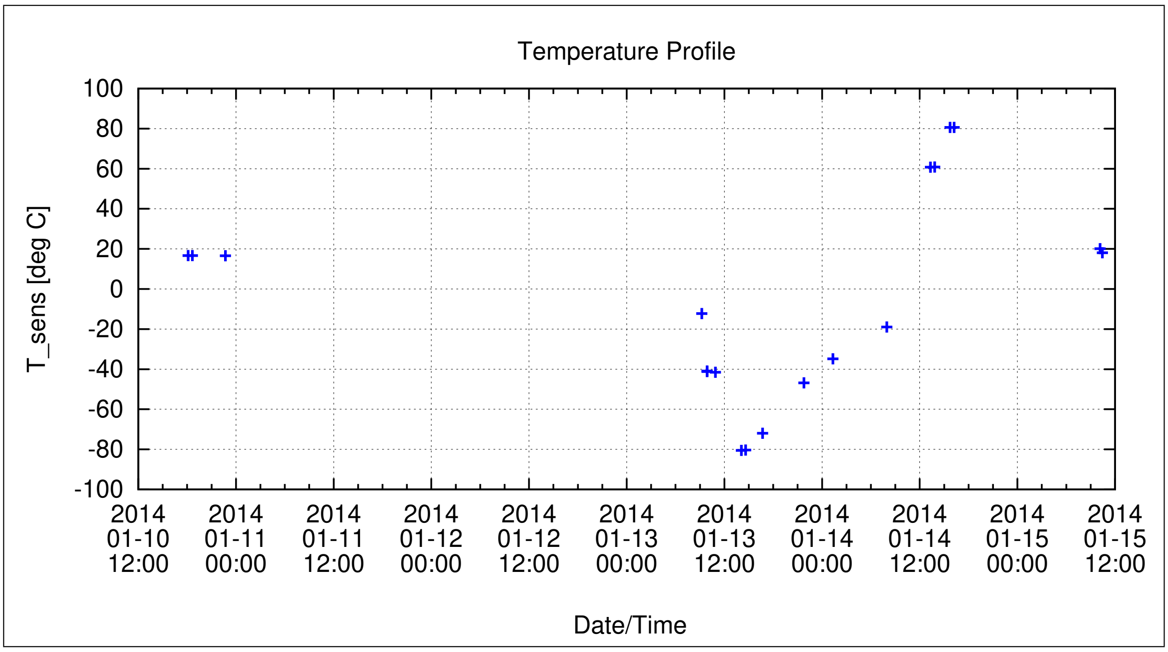

Figure 47: Temperature Profile

Calibration Parameter:

Sensitivity σ_i vs. Temperature:

$$\sigma_i(T) = \sum_{k=0}^{n} \sigma_{k,i} T^k \qquad [1,\ ^\circ\mathrm{C}],\ \mathrm{i=\{x,y,z\}}$$

	$\sigma_{0,i}$	$\sigma_{1,i}$	$\sigma_{2,i}$	$\sigma_{3,i}$	$\sigma_{4,i}$	$\sigma_{5,i}$
σ_x	9.98815E-1	-1.78666E-5				
σ_y	9.99394E-1	-1.34155E-5				
σ_z	9.99098E-1	-1.81212E-5				

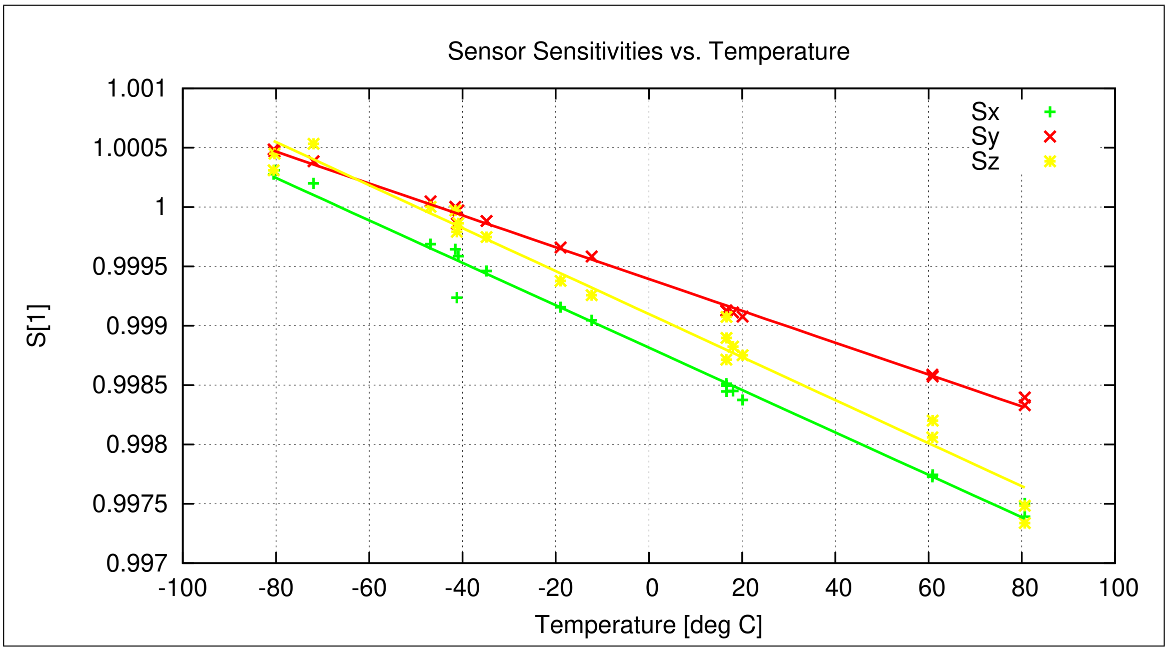

Figure 48: Temperature dependence of Sensitivities

Misalignment Angles ξ_{ij} vs. Temperature:

$$\xi_{ij}(T) = \sum_{k=0}^{n} \xi_{k,ij} T^k \qquad [\text{deg}, \ ^\circ\text{C}], \ \text{ij}= \{\text{xy,xz,yz}\}$$

	$\xi_{0,ij}$	$\xi_{1,ij}$	$\xi_{2,ij}$	$\xi_{3,ij}$	$\xi_{4,ij}$	$\xi_{5,ij}$
ξ_{xy}	8.9684E+1	-1.0371E-5				
ξ_{xz}	8.9717E+1	6.9566E-5				
ξ_{yz}	9.0113E+1	2.1981E-5				

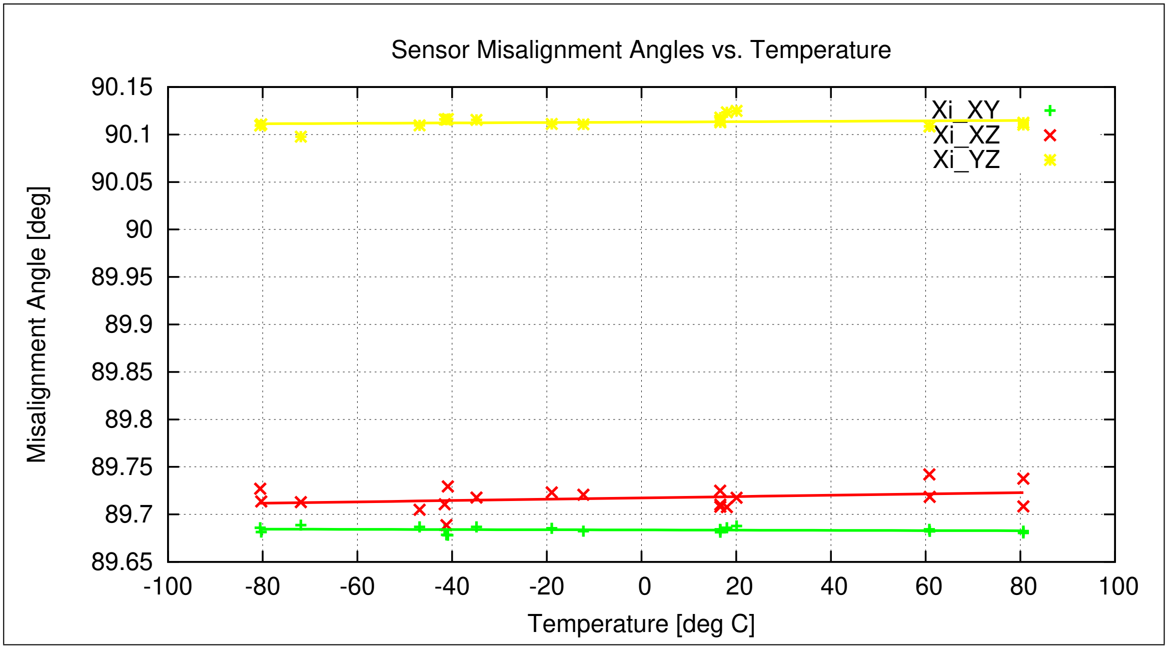

Figure 49: Temperature dependence of Misalignment Angles

Offset & Residual MCF Field $\underline{B}^{or} = \underline{B}^{off} + \underline{B}^{res}$ vs. Temperature:

$$\underline{B}^{or}(T) = \sum_{k=0}^{n} \underline{B}_k^{or} T^k \qquad [\text{enT, °C}]$$

	$\underline{B}_0^{or}$	$\underline{B}_1^{or}$	$\underline{B}_2^{or}$	$\underline{B}_3^{or}$	$\underline{B}_4^{or}$	$\underline{B}_5^{or}$
B_x^{or}	2.220E+1	3.617E-2				
B_y^{or}	1.240E+1	-3.514E-4				
B_z^{or}	-4.415E+0	5.270E-2				

Model Quality:

Minimum and maximum errors of the calculated Model vs. Temperature:

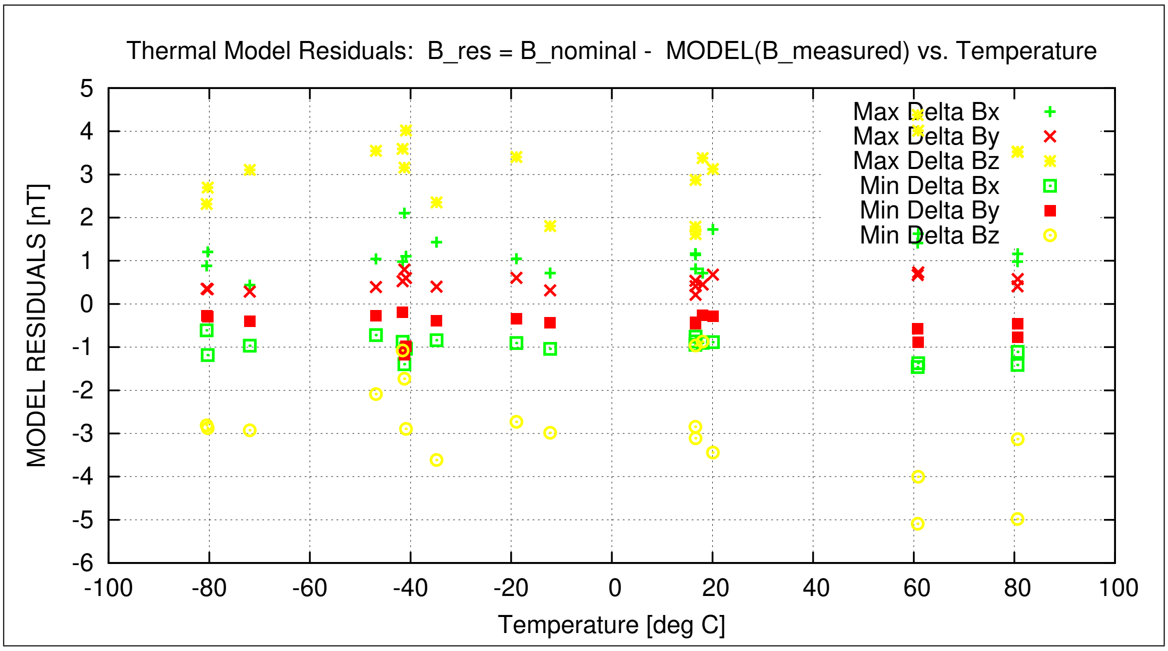

Figure 50: Residuals of Thermal Model

Sensor Rotation during Test:

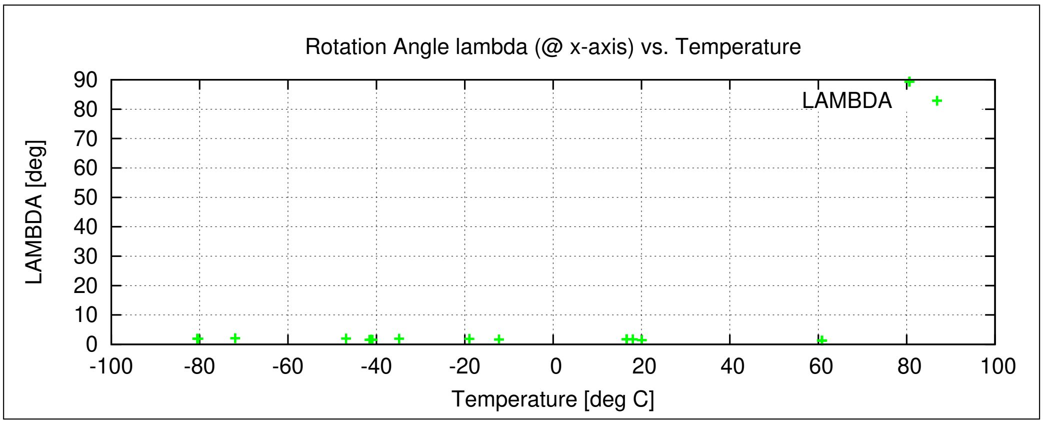

Figure 51: Rotation @ X-Axis

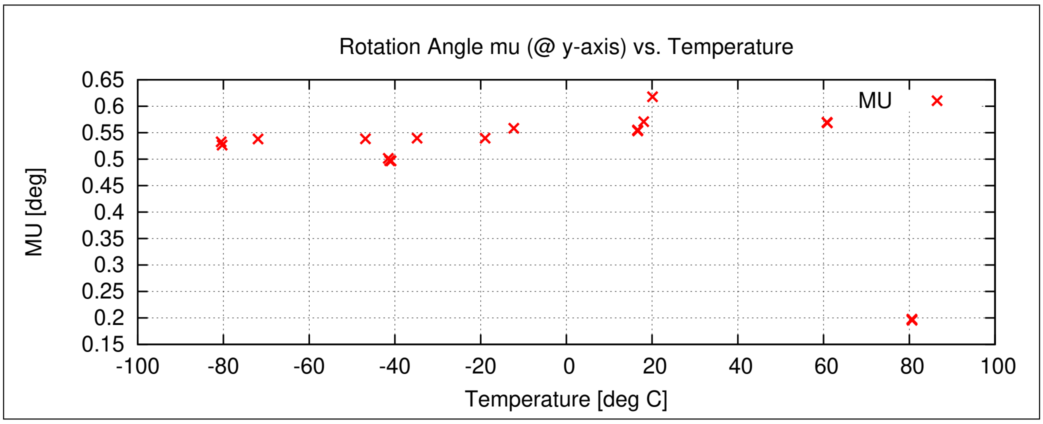

Figure 52: Rotation @ Y-Axis

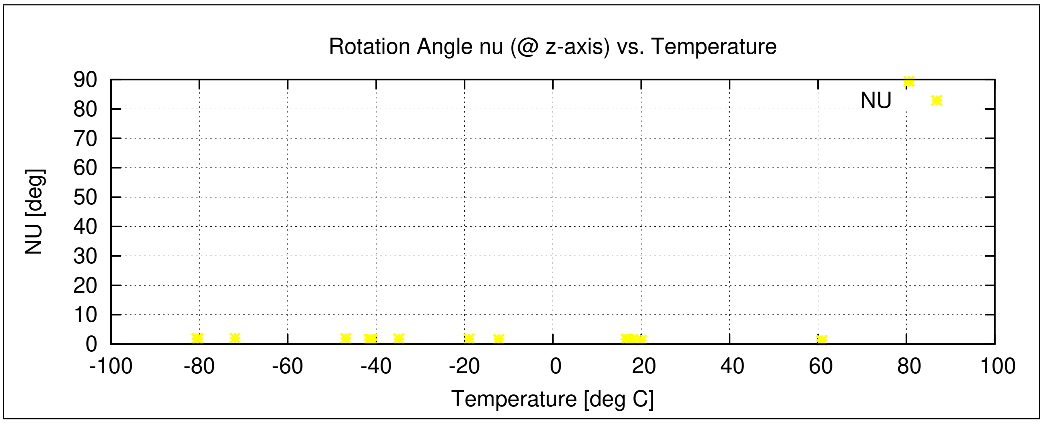

Figure 53: Rotation @ Z-Axis

8.1.2 Temperature Calibration of the Sensor Offset

Used Temperature Measurements:

Calibration Parameter File	Remark
OFF_PARAMETER__14-01-10-16-25-52.OPF	
OFF_PARAMETER__14-01-13-08-43-55.OPF	
OFF_PARAMETER__14-01-13-10-25-04.OPF	
OFF_PARAMETER__14-01-13-14-10-49.OPF	
OFF_PARAMETER__14-01-14-07-41-16.OPF	
OFF_PARAMETER__14-01-14-10-24-51.OPF	
OFF_PARAMETER__14-01-14-13-21-06.OPF	
OFF_PARAMETER__14-01-14-15-44-27.OPF	
OFF_PARAMETER__14-01-15-11-08-47.OPF	

Thermal Parameter File: THERMAL_OFF_PARAMETER__14-01-10-16-25-52.TOF

Facility Parameter:

Nominal Sensor Setup $\underline{B}_{\mathrm{DUT}} = \underline{\underline{R}}_{\mathrm{nom}} \underline{B}_{\mathrm{c}}$

$$\underline{\underline{R}}_{\mathrm{nom}} = \begin{pmatrix} +1.000000 & +0.000000 & +0.000000 \\ +0.000000 & +1.000000 & +0.000000 \\ +0.000000 & +0.000000 & +1.000000 \end{pmatrix}$$

Sensor Temperature Channel: T_{59}

Coil System Temperature Channel: T_{29}

Temperature Profile

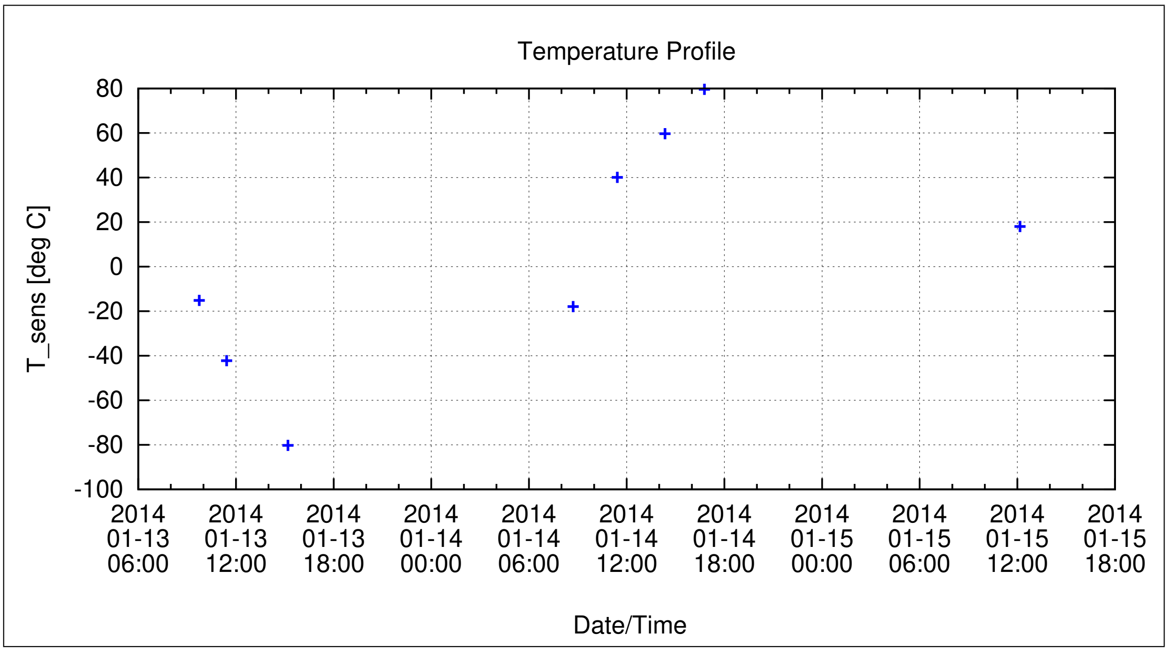

Figure 54: Temperature Profile

Calibration Parameter:

Sensor Offset $\underline{B}_{\rm off}$ vs. Temperature:

$$B_{\rm off,i}(T) = \sum_{k=0}^{n} B_{\rm off,k,i} T^k \qquad [\text{enT}, \ ^\circ\text{C}], \ \text{i}=\{\text{x,y,z}\}$$

	$B_{\rm off,0,i}$	$B_{\rm off,1,i}$	$B_{\rm off,2,i}$	$B_{\rm off,3,i}$	$B_{\rm off,4,i}$	$B_{\rm off,5,i}$
$B_{\rm off,x}$	1.76453E+1	-1.25373E-2				
$B_{\rm off,y}$	1.46506E+1	5.57159E-3				
$B_{\rm off,z}$	4.06089E+0	-6.07191E-3				

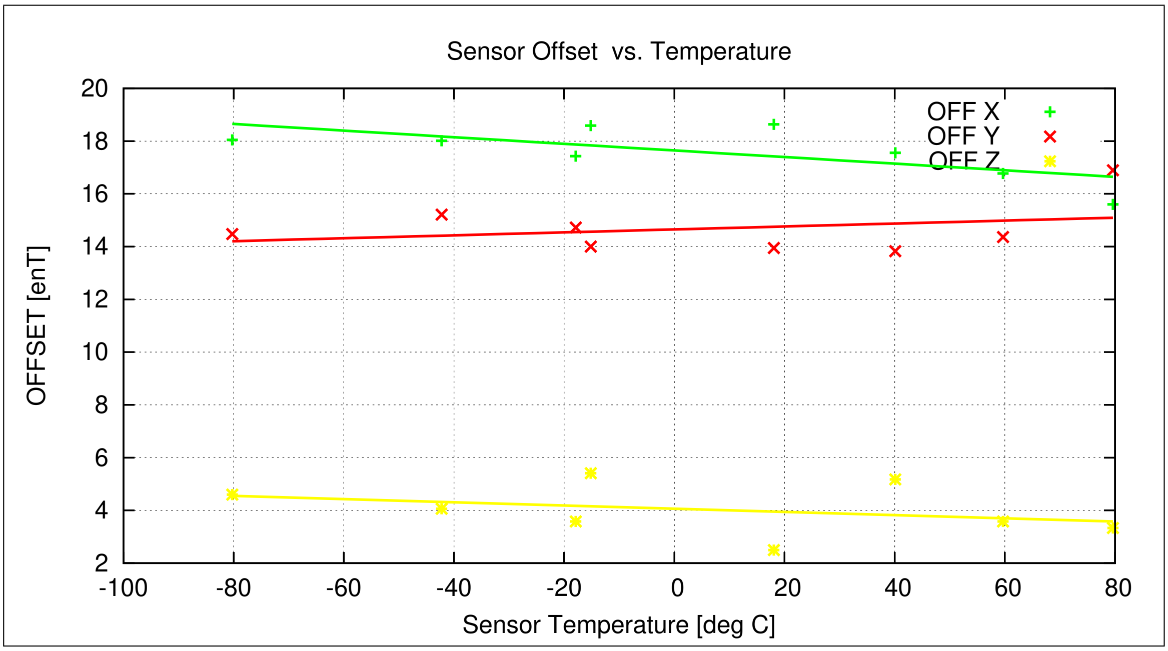

Figure 55: Temperature dependence of Sensor Offsets

Coil System Temperature

The following graph shows the mean Coil System temperature during the complete thermal cycle for the offset measurements.

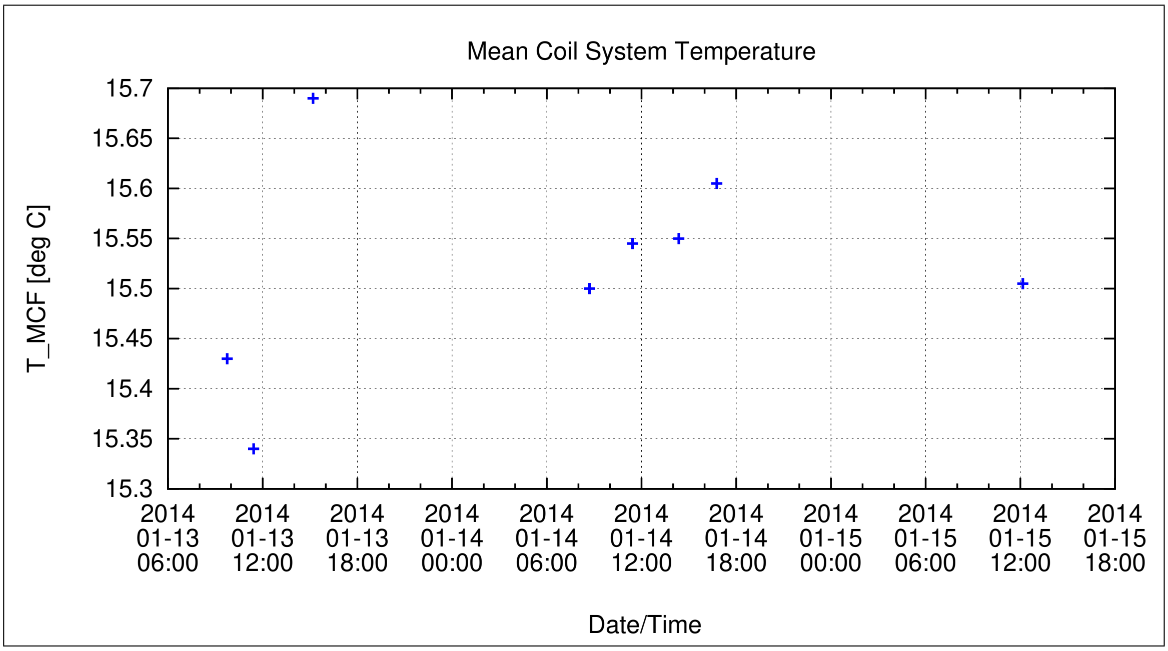

Figure 56: Coil System Temperature during Thermal Measurements

Coil System Residual Field:

The following graph shows the three components of the Coil System Residual field during the whole measurement. Axes designators are related to the actual DUT coordinate system and NOT to Coil System coordinates.

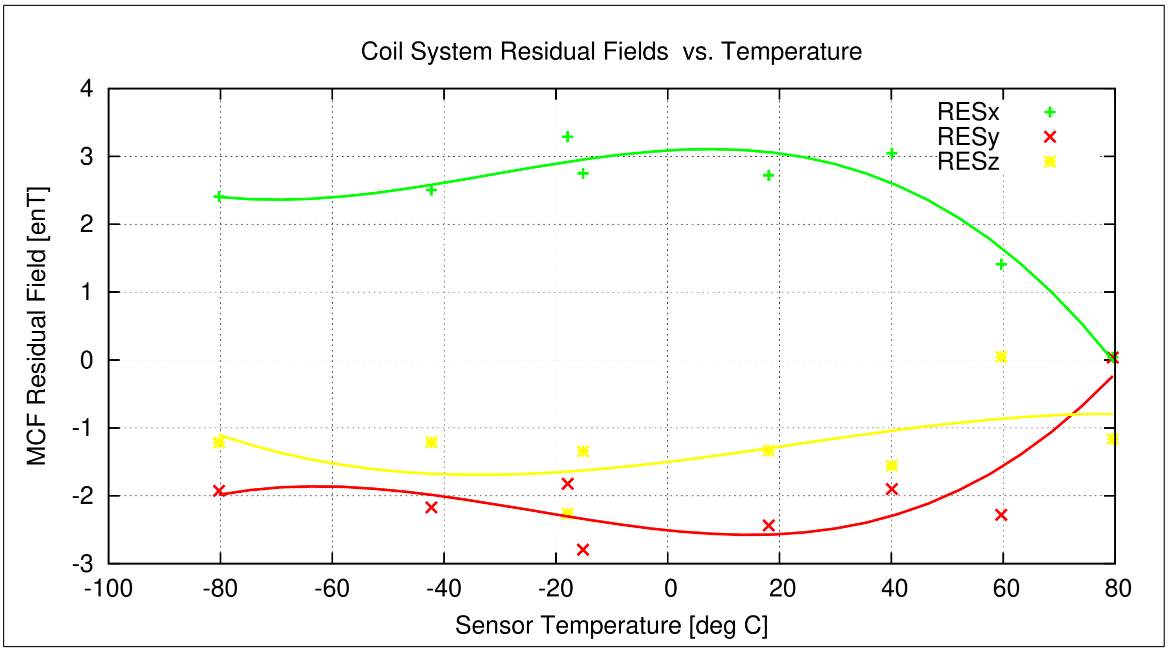

Figure 57: Coil System Residual Fields during Thermal Measurements

Remark:

The axes designation for this graph is given as follows (rf. to setup defined in chapter 1):

$$X_m = X_c$$
$$Y_m = Y_c$$
$$Z_m = -X_c$$

8.1.3 Temperature Calibration of the AC Transfer Function

Used Temperature Measurements:

Calibration Parameter File	Remark
FREQ_PARAMETER__14-01-10-15-43-38.FPF	
FREQ_PARAMETER__14-01-14-10-32-56.FPF	
FREQ_PARAMETER__14-01-14-13-28-50.FPF	
FREQ_PARAMETER__14-01-14-15-57-46.FPF	
FREQ_PARAMETER__14-01-15-09-42-36.FPF	

Thermal Parameter File: THERMAL_AC_PARAMETER__14-01-10-15-43-38.TAF

Facility Parameter:

Nominal Sensor Setup: Diagonal in Space inside Thermal Box.

Sensor Temperature Channel: T_{59}

Coil System Temperature Channel: T_{29}

Temperature Profile

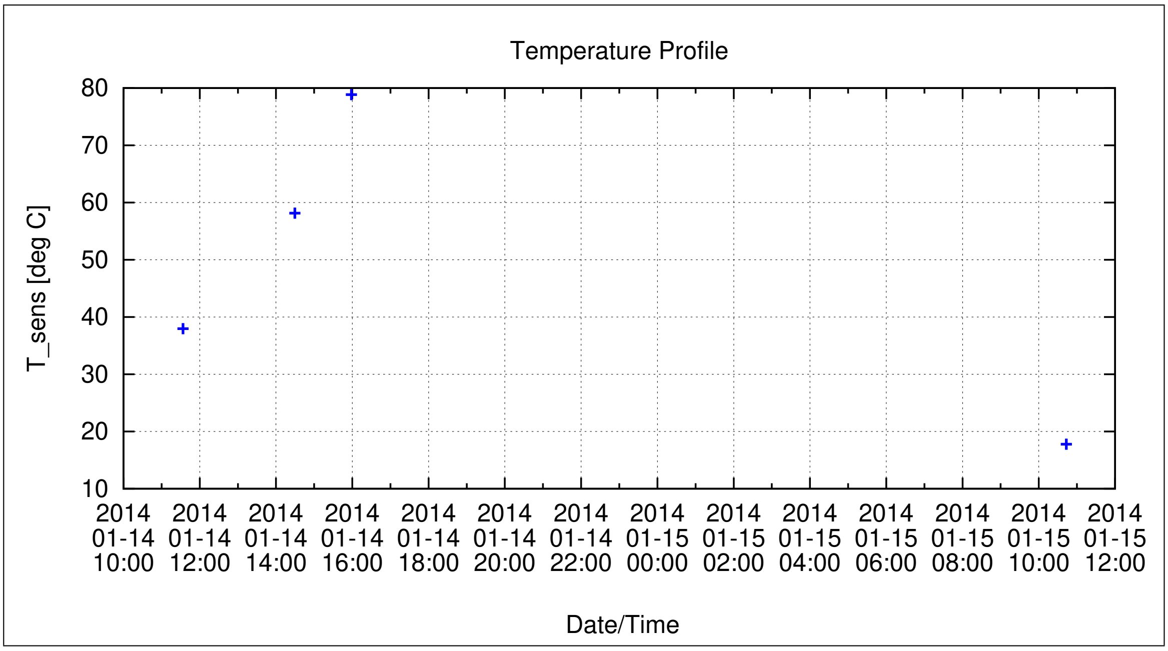

Figure 58: Temperature Profile

Coil System Temperature

The following graph shows the mean Coil System temperature during the complete thermal cycle for the AC measurements.

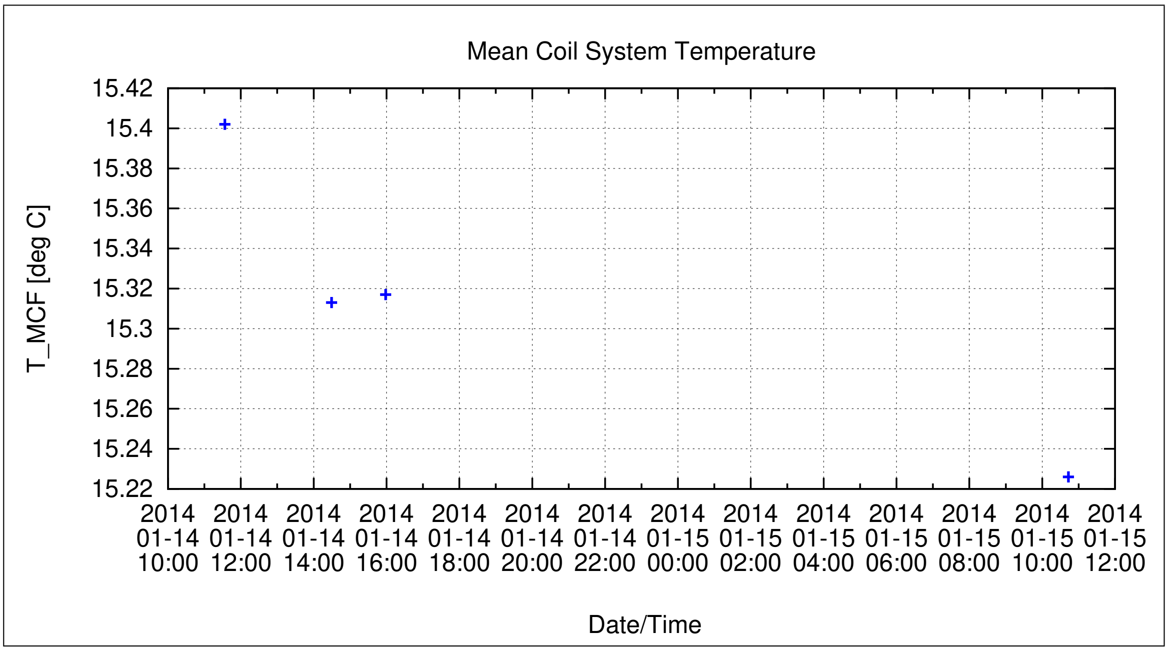

Figure 59: Coil System Temperature during Thermal AC Measurements

Calibration Parameter:

-3dB Corner Frequency $f_{3\mathrm{dB}}$ vs. Temperature:

$$f_{3\mathrm{dB,i}}(T) = \sum_{k=0}^{n} f_{3\mathrm{dB,k,i}} T^k \qquad [\mathrm{Hz},\ ^\circ\mathrm{C}],\ \mathrm{i}=\{\mathrm{x,y,z}\}$$

	$f_{3\mathrm{dB,0,i}}$	$f_{3\mathrm{dB,1,i}}$	$f_{3\mathrm{dB,2,i}}$	$f_{3\mathrm{dB,3,i}}$	$f_{3\mathrm{dB,4,i}}$	$f_{3\mathrm{dB,5,i}}$
$f_{3\mathrm{dB,x}}$	5.47776E+0	-6.74126E-3				
$f_{3\mathrm{dB,y}}$	5.36743E+0	-4.05430E-3				
$f_{3\mathrm{dB,z}}$	5.44671E+0	-5.38190E-3				

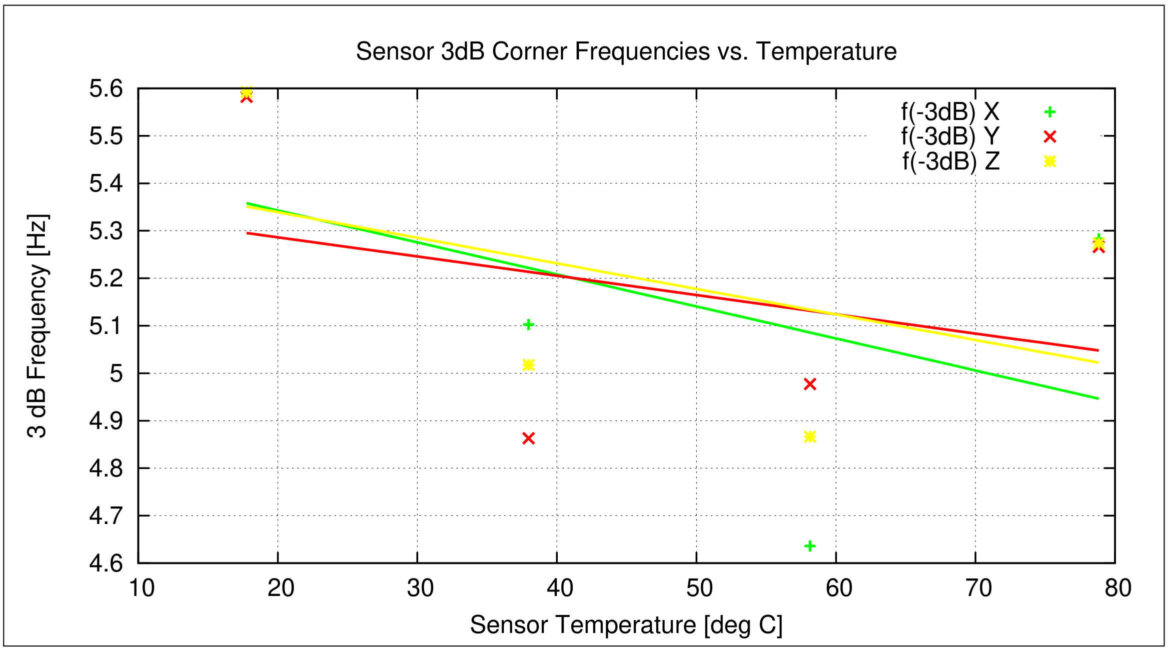

Figure 60: Temperature dependence of 3dB Corner Frequency

Instrument Sampling Frequency:

The following graph shows the calculated sampling frequencies vs. the actual sensor temperature.

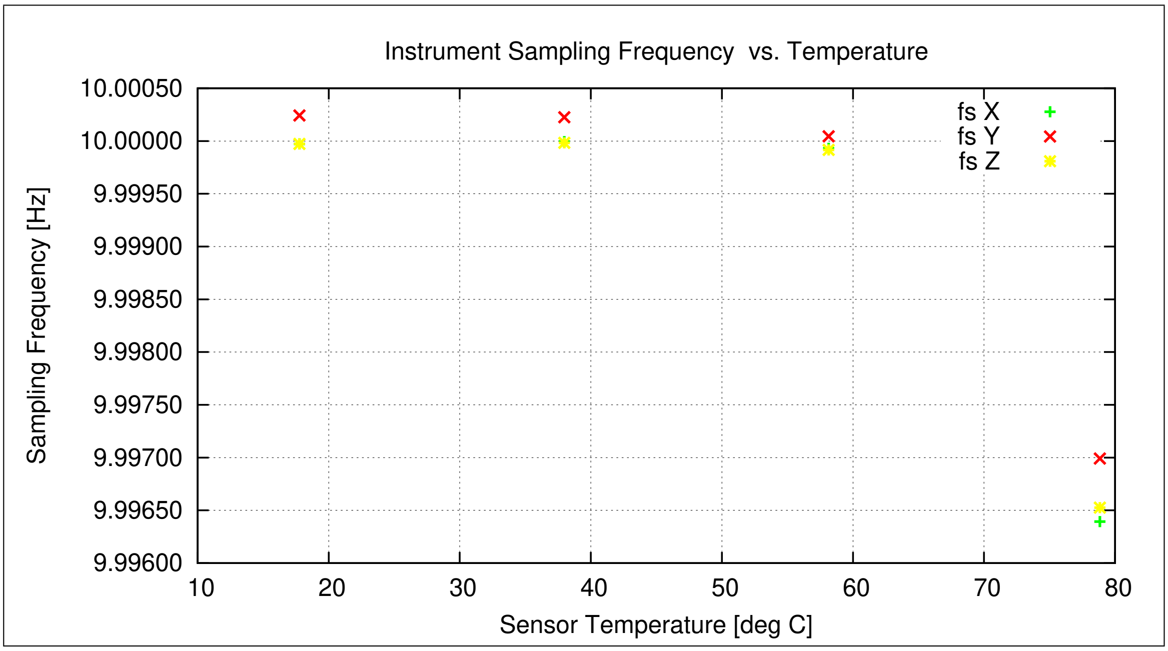

Figure 61: Instrument Sampling Frequency versus Sensor Temperature

Mean Samplerate: 9.999182 Hz.
Mean Standard Deviation of Samplerate: 0.001698 Hz.

8.2 Complete Temperature Profile

The following plot shows the complete thermal cycle of the sensor with all cooling and heating phases. The curves show the desired nominal temperatures in green and the actual measured temperatures in red.

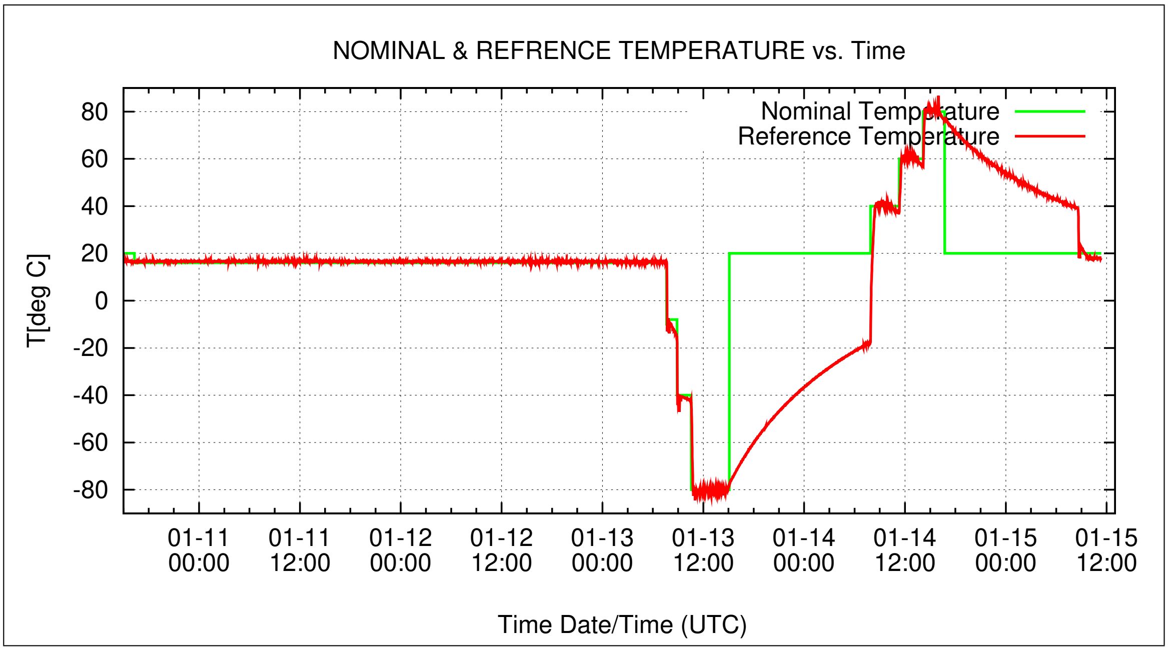

Figure 62: Complete thermal cycle

9 Mathematical Description of the Calibration

9.1 Basic Principle

The Magnetsrode Coil Facility (MCF) generates an artificial magnetic field $\underline{B}^{\mathrm{FLD}}$ that can be considered as a calibrated, orthogonal magnetic reference field[1] defined in coilsystem coordinates. For the calibration analysis this ideal coilsystem field is rotated to ideal orthogonal sensor coordinates using a nominal Rotation matrix $\underline{\underline{R}}_{\mathrm{nom}}$ at the first step. Nominal means that only rotations of ±90° or ±180° at any axis are considered here to get a coarse alignment of the applied field with the sensor-axes.

$$\underline{B}^{\mathrm{c}} = \underline{\underline{R}}_{\mathrm{nom}}\, \underline{B}^{\mathrm{FLD}}$$

For a standard calibration the matrix $\underline{\underline{R}}_{\mathrm{nom}}$ is just a $\underline{\underline{I}}$ - matrix - sensor coordinates and coilsystem coordinates have roughly the same direction. If the sensor coordinates are left-handed or the sensor is turned by about ±90° or ±180° at any axis $\underline{\underline{R}}_{\mathrm{nom}}$ will contain ±1-elements or 0-elements at any place. The rotated coil system field $\underline{B}^{\mathrm{c}}$ is the used reference field for the following analysis.

The magnetometer under test at the center of the coil system (CoC) generates magnetic raw data $\underline{B}^{\mathrm{r}}$. These data include an eventually existing residual field of the coil system $\underline{B}^{\mathrm{res}}$ and the magnetometer offset $\underline{B}^{\mathrm{off}}$. Both entities are combined in the offset & residual field $\underline{B}^{\mathrm{or}}$:

$$\underline{B}^{\mathrm{or}} = \underline{B}^{\mathrm{off}} + \underline{B}^{\mathrm{res}}$$

Therefore, the second step of the calibration is the generation of offset and residual field corrected measured field data $\underline{B}^{\mathrm{m}}$:

$$\underline{B}^{\mathrm{m}} = \underline{B}^{\mathrm{r}} - \underline{B}^{\mathrm{or}}$$

The actual offset and residual field is automatically taken into account during the calibration analysis. Either a constant field or - if needed - a linear trend of $\underline{B}^{\mathrm{or}}$ is subtracted from the raw data.

The relation between the calibration field and the magnetometer data is then defined by

$$\underline{B}^{\mathrm{c}} = \underline{\underline{\Phi}}\, \underline{B}^{\mathrm{m}}$$

where $\underline{\underline{\Phi}}$ is the complete calibration transfer matrix, defined by

$$\underline{\underline{\phi}} = \underline{\underline{R}}_{\mathrm{nom}}\ \underline{\underline{\rho}}\, \underline{\underline{\omega}}\, \underline{\underline{\sigma}}.$$

[1] During the calibration the temperature dependent sensitivity of the coil system is calculated every 3 minutes and taken into account as well as the static misalignment of the coil system to produce orthogonal, known fields.

$\underline{\underline{\sigma}}(T)$ represents the temperature dependent sensitivity.
$\underline{\underline{\omega}}(T)$ describes the temperature dependent internal sensor misalignment (orthogonalisation matrix).
$\underline{\underline{\rho}}(T)$ describes the real rotation of the sensor against the coil axes.[2]

Thus the calibration algorithms have to solve the following problem:

$$\begin{aligned} \underline{B}^{\mathrm{c}} &= \underline{\underline{\Phi}}\ \underline{B}^{\mathrm{m}} \\ &= \underline{\underline{R}}_{\mathrm{nom}}\ \underline{\underline{\rho}}\ \underline{\underline{\omega}}\ \underline{\underline{\sigma}}\ \underline{B}^{\mathrm{m}} \end{aligned} \tag{1}$$

The separation into these submatrices and evaluation of their elements is done in subsequent steps:

- Calculation of the Sensitivity matrix $\underline{\underline{\sigma}}$
  The sensitivity matrix shall contain the on-axis sensitivity coefficients of the sensors. Therefore, $\underline{\underline{\sigma}}$ has to be a diagonal matrix of the following kind:

  $$\underline{\underline{\sigma}} = \begin{pmatrix} \sigma_1 & 0 & 0 \\ 0 & \sigma_2 & 0 \\ 0 & 0 & \sigma_3 \end{pmatrix}$$

  The separation of matrix $\underline{\underline{\sigma}}$ from the transfer function $\underline{\underline{\phi}}$ yields

  $$\underline{\underline{\phi}} = \begin{pmatrix} \frac{\phi_{11}}{\sigma_1} & \frac{\phi_{12}}{\sigma_2} & \frac{\phi_{13}}{\sigma_3} \\ \frac{\phi_{21}}{\sigma_1} & \frac{\phi_{22}}{\sigma_2} & \frac{\phi_{23}}{\sigma_3} \\ \frac{\phi_{31}}{\sigma_1} & \frac{\phi_{32}}{\sigma_2} & \frac{\phi_{33}}{\sigma_3} \end{pmatrix} \begin{pmatrix} \sigma_1 & 0 & 0 \\ 0 & \sigma_2 & 0 \\ 0 & 0 & \sigma_3 \end{pmatrix} := \underline{\underline{\hat{\phi}}}\ \underline{\underline{\sigma}}$$

  For the computation of the sensitivity coefficients σ_i the transformation of the basevectors has to be considered. Equation (1) transform the components of the fields, whereas

  $$\underline{e}^{\mathrm{c}} = \left(\underline{\underline{\phi}}^{\mathrm{T}}\right)^{-1}\ \underline{e}^{\mathrm{m}} := \underline{\underline{\Psi}}\ \underline{e}^{\mathrm{m}}$$

  has to be used for the contragredient base-vector transformation of the skew sensorsystem Σ^{m} into the orthonormal coilsystem Σ^{c}. The length of the column vectors of $\underline{\underline{\psi}}$ define the sensitivity coefficients σ_i:

  $$\sigma_1 = \frac{1}{\sqrt{\psi_{11}^2 + \psi_{21}^2 + \psi_{31}^2}}$$

[2] Also the rotation matrix is regarded as temperature dependent being able to consider any thermal setup inadequacies causing fractional rotations.

$$\sigma_2 = \frac{1}{\sqrt{\psi_{12}^2 + \psi_{22}^2 + \psi_{32}^2}}$$
$$\sigma_3 = \frac{1}{\sqrt{\psi_{13}^2 + \psi_{23}^2 + \psi_{33}^2}}$$

- Calculation of the Misalignment matrix $\underline{\underline{\omega}}$

  After the separation of $\underline{\underline{\sigma}}$ the reduced transfer function $\overset{\wedge}{\underline{\underline{\phi}}}$ contains only the misalignment and the real sensor rotation. The misalignment angles $\xi_{xy}, \xi_{xz}, \xi_{yz}$, hence the angles between the base vectors of the affine sensorsystem Σ^{m}, can be evaluated from the scalar products of all these base vectors. The base unit vectors are defined by the inverse transposed matrix of the reduced transfer function:

$$\underline{e}_{\mathrm{x}}^{\mathrm{m}} := \left(\overset{\wedge}{\underline{\underline{\phi}}}^{\mathrm{T}}\right)^{-1} \begin{pmatrix} 1 \\ 0 \\ 0 \end{pmatrix}$$
$$\underline{e}_{\mathrm{y}}^{\mathrm{m}} := \left(\overset{\wedge}{\underline{\underline{\phi}}}^{\mathrm{T}}\right)^{-1} \begin{pmatrix} 0 \\ 1 \\ 0 \end{pmatrix}$$
$$\underline{e}_{\mathrm{z}}^{\mathrm{m}} := \left(\overset{\wedge}{\underline{\underline{\phi}}}^{\mathrm{T}}\right)^{-1} \begin{pmatrix} 0 \\ 0 \\ 1 \end{pmatrix}$$

  The misalignment angles can be derived from the scalar products:

$$\xi_{xy} = \arccos\left(\underline{e}_x^m \cdot \underline{e}_y^m\right)$$
$$\xi_{xz} = \arccos\left(\underline{e}_x^m \cdot \underline{e}_z^m\right)$$
$$\xi_{yz} = \arccos\left(\underline{e}_y^m \cdot \underline{e}_z^m\right)$$

  Let's assume that the x-axis of the reference system $\underline{e}_{\mathrm{x}}^{\mathrm{c}}$ is identical to the $\underline{e}_{\mathrm{x}}^{\mathrm{m}}$-axis of the sensor system. The angle between $\underline{e}_{\mathrm{y}}^{\mathrm{c}}$ and $\underline{e}_{\mathrm{y}}^{\mathrm{m}}$ is β (rotation angle around the $\underline{e}_{\mathrm{z}}^{\mathrm{c}}$ axis). And the sensor $\underline{e}_{\mathrm{z}}^{\mathrm{m}}$ axis can be constructed by a rotation of η in the $\underline{e}_{\mathrm{x}}^{\mathrm{c}}, \underline{e}_{\mathrm{y}}^{\mathrm{c}}$-plane and a second rotation of γ out of this plane. Then this misalignment of the base vectors is given by

$$\underline{\underline{O}} = \begin{pmatrix} 1 & \sin\beta & \sin\gamma \\ 0 & \cos\beta & \cos\gamma\sin\eta \\ 0 & 0 & \cos\gamma\cos\eta \end{pmatrix} \qquad (2)$$

  By comparison of the angles β, η, γ with misalignment angles $\xi_{xy}, \xi_{xz}, \xi_{yz}$, the misalignment matrix (2) can be written in the following shape:

$$\underline{\underline{O}} = \begin{pmatrix} 1 & \cos\xi_{xy} & \cos\xi_{xz} \\ 0 & \sin\xi_{xy} & \dfrac{\cos\xi_{yz} - \cos\xi_{xy}\cos\xi_{xz}}{\sin\xi_{xy}} \\ 0 & 0 & \sqrt{\sin^2\xi_{xz} - \dfrac{(\cos\xi_{yz} - \cos\xi_{xy}\cos\xi_{xz})^2}{\sin^2\xi_{xy}}} \end{pmatrix}$$

$\underline{\underline{O}}$ transforms the base vectors. To achieve the transformation between the field components the transposed, inverse matrix of $\underline{\underline{O}}$ has to be calculated as the final misalignment matrix:

$$\underline{\underline{\omega}} = \left(\underline{\underline{O}}^{\mathrm{T}}\right)^{-1}$$

- Calculation of the Rotation matrix $\underline{\underline{\rho}}$
  With the knowledge of $\underline{\underline{\omega}}$ and the nominal Setup matrix $\underline{\underline{R}}_{\mathrm{nom}}$ the rotation matrix $\underline{\underline{\rho}}$ can be evaluated:

$$\underline{\underline{\rho}} = (\underline{\underline{R}}_{\mathrm{nom}})^{-1} \ \underline{\underline{\hat{\phi}}} \ (\underline{\underline{\omega}})^{-1}$$

  From this rotation matrix the actual rotation angles of the sensor wrt. the coil system can be calculated using again the scalar product:

$$\begin{aligned} \lambda &:= \arccos\left(\left[\underline{\underline{\rho}}\begin{bmatrix}1\\0\\0\end{bmatrix}\right] \cdot \begin{bmatrix}1\\0\\0\end{bmatrix}\right) \\ \mu &:= \arccos\left(\left[\underline{\underline{\rho}}\begin{bmatrix}0\\1\\0\end{bmatrix}\right] \cdot \begin{bmatrix}0\\1\\0\end{bmatrix}\right) \\ \nu &:= \arccos\left(\left[\underline{\underline{\rho}}\begin{bmatrix}0\\0\\1\end{bmatrix}\right] \cdot \begin{bmatrix}0\\0\\1\end{bmatrix}\right) \end{aligned}$$

  The rotation matrix $\underline{\underline{\rho}}$ and the rotation angles λ, μ, ν are of interest just for the calibration to determine the right magnetometer parameters.

The transfer function for the normal use of the magnetometer is just given by

$$\underline{\underline{\tilde{\phi}}} = \underline{\underline{\omega}} \ \underline{\underline{\sigma}}$$

10 Nomenclature

Abbreviations in theoretical sections:

Item	Meaning
$\underline{B}^c$	Magnetic calibration field generated by coil system
$\underline{B}^{off}$	Offset of the magnetometer [nT]
$\underline{B}_k^{off}$	Polynomial Fit coefficients for the sensor offset vs. temperature
$\underline{B}^m$	Measured magnetic field raw data, offset & residual field corrected [nT]
$\underline{B}^{or}$	$= \underline{B}^{off} + \underline{B}^{res}$, Offset + Residual field at CoC [enT]
$\underline{B}^r$	Magnetic field raw data
$B^r_{0°}$	Magnetic raw data, measured in normal position (0°)[enT]
$B^r_{180°}$	Magnetic raw data, measured in turned position (180°)[enT]
$\underline{B}^{res}$	Residual field of the coil system
e°C	Engineering degrees centigrade units
enT	Engineering NanoTesla units
c_0, c_1, c_2, c_3	Fit coefficients of the sensor thermistor
i	component x | y | z
CoC	Center of Coil system
DUT	Device under Test
$\underset{\sim}{\underline{\underline{\phi}}}$	$= \underline{\underline{R}}_{\text{nom}}\,\underline{\underline{\rho}}\,\underline{\underline{\omega}}\,\underline{\underline{\sigma}}$, Calibration Transfer Matrix
$\underline{\underline{\phi}}$	$= \underline{\underline{\omega}}\,\underline{\underline{\sigma}}$, Transfer Matrix
$\hat{\underline{\underline{\phi}}}$	$= \underline{\underline{\phi}}\,\underline{\underline{\sigma}}^{-1}$, Reduced Transfer Matrix
$\underline{\underline{\psi}}$	$= (\underline{\underline{\phi}}^T)^{-1}$, Auxilliary transfer matrix
$\underline{\underline{O}}$	Base vector Orthogonalisation matrix
$\underline{\underline{\omega}}$	$= (\underline{\underline{O}}^T)^{-1}$, Field components orthogonalisation matrix
$\underline{\underline{R}}_{\text{nom}}$	Nominal Rotation matrix of sensor vs. coil system
$\underline{\underline{\rho}}$	= Actual rotation matrix
$\underline{\underline{\sigma}}$	= Sensitivity matrix
$\sigma_{k,i}$	Polynomial Fit coefficient for sensitivity vs. temperature. Coefficient of order k for the sensor component i
TeMeSys	MRode Temperature Measurement System
T_s^c	Temperature of sensor s, calibrated data [°C]
T_s^r	Temperature of sensor s, raw data [e°C]
s	Sensor IB | OB
$U_{\text{T, IB}}$	IB–Temperature data [V], measured
$U_{\text{T,OB}}$	OB–Temperature data [V], measured
ξ_{ij}	Temperature dependent alignment angle (ij component)
$\xi^0_{k,ij}$	Polynomial Fit coefficient for misalignment angle vs. temperature. Coefficient of order k for the angle ij
λ, μ, ν	Rotation angles wrt. coil system reference coordinates.